CHARACTERIZING NEAR-ROAD AIR POLLUTION USING LOCAL-SCALE EMISSION AND DISPERSION MODELS AND VALIDATION AGAINST IN-SITU MEASUREMENTS

An Wang

Department of Civil Engineering & Applied Mechanics
McGill University, Montreal
April 2016

A thesis submitted to McGill University in partial fulfillment of the requirements of the degree of Master of Engineering in Civil Engineering

TABLE OF CONTENTS

ABSTRACT....................iv

RÉSUMÉ....................vi

LIST OF FIGURES....................viii

LIST OF TABLES....................ix

LIST OF ABBREVIATIONS....................x

ACKNOWLEDGEMENTS....................xi

PREFACE AND CONTRIBUTION OF AUTHORS....................xii

CHAPTER 1 INTRODUCTION....................1

1.1 Background and Motivation....................1

1.2 Objectives....................3

1.3 Summary....................3

CHAPTER 2 INTEGRATION OF TRAFFIC SIMULATION, EMISSION ESTIMATION AND DISPERSION MODELING: STATE OF THE ART AND PRACTICE....................6

2.1 Introduction....................6

2.2 Traffic-Related Air Pollution and Health....................6

2.3 Air Pollution Dispersion Modeling....................9

2.4 Validation and Comparison between Dispersion Models....................11

2.5 Contributions....................13

2.6 Conclusion....................13

CHAPTER 3 DATA COLLECTION METHODOLOGY....................15

3.1 Introduction....................15

3.2 *In-situ* Data Collection....................15

3.2.1 Corridor Selection....................15

3.2.2 Instruments....................17

3.2.3 Data Collection Protocol....................20

3.3 Fixed-station Data Collection....................23

3.3.1 Meteorological Data....................23

3.3.2 NO_2 Concentrations....................23

3.3.3 Land Use Data Collection....................24

3.4 Conclusion 25

CHAPTER 4 DATA PROCESSING..26

4.1 Introduction..26

4.2 Traffic Data Processing..26

4.2.1 Manual Traffic Counts..26

4.2.2 Traffic Counting Results..29

4.3 Meteorological Data Synchronization 30

4.4 NO_2 Data Processing..34

4.4.1 NO_2 Data Cleaning and Synchronization 34

4.4.2 Descriptive Results for Measured NO_2 Concentrations 36

4.5 Conclusion 38

CHAPTER 5 TRAFFIC SIMULATION AND EMISSION COMPUTATION 39

5.1 Introduction..39

5.2 Traffic Simulation..39

5.2.1 Traffic Simulation Purpose and Procedures 39

5.2.2 Traffic Simulation Network...41

5.2.3 Organization of Traffic Simulation Inputs..42

5.3 Emission Calculation 43

5.3.1 Total Emissions...43

5.3.2 Emission Factor Calculation 45

5.4 Conclusion 45

CHAPTER 6 DISPERSION MODELING USING OSPM, CALINE4 AND SIRANE AND MODEL PERFORMANCE VALIDATION AND COMPARISON 46

6.1 Introduction..46

6.2 OSPM Dispersion Modeling...46

6.2.1 Introduction to OSPM..46

6.2.2 Universal Inputs 48

6.2.3 OSPM Featured Inputs...48

6.3 CALINE4 Dispersion Modeling...49

6.4 SIRANE Dispersion Modeling 51

6.5 Validation and Inter-Comparison of Dispersion Models..52

6.6 Conclusion 54

CHAPTER 7 RESULTS AND DISCUSSIONS..55
7.1 Introduction..55
7.2 Traffic Simulation and Emission Calculation..55
7.2.1 Traffic Simulation Results...55
7.2.2 Emission Calculation Results..58
7.3 Dispersion Modeling Results...58
7.4 Dispersion Modeling Validation and Inter-comparison Results....................................60
7.5 Discussion...63
7.5.1 Fixed-station and Roadside Measurements...63
7.5.2 Dispersion Model Performance at Different Locations...64
7.5.3 Dispersion Model Performance under Different Meteorological Conditions.........65
7.6 Conclusion..66

CHAPTER 8 CONCLUSION 68
8.1 Summary...68
8.2 Implications..69
8.3 Limitations and Future Work..70

REFERENCES 72

ABSTRACT

Traffic-related air pollution has been widely considered to be significantly associated with chronic and acute adverse health effects in urban environments. Since high-density traffic emits a considerable amount of pollutants, which are often trapped within urban canyons, individuals living in these areas are exposed to higher levels of traffic-related air pollution. A marked trend towards increasing global urbanization highlights the importance of understanding the patterns of traffic-related air pollution dispersion and recirculation and identifying a proper methodology to reproduce them.

The objective of this thesis includes two main components: 1) the integration of microscopic traffic simulation, emission computation and dispersion modeling that reproduces air pollution recirculation patterns in urban environments, and 2) estimation, validation and comparison between different dispersion algorithms.

In order to fulfill these objectives, near-road concentrations of nitrogen dioxide (NO_2), a known marker of traffic-related air pollution, were simulated along a busy urban corridor in Montreal, Canada using a combination of microscopic traffic simulation, instantaneous emission modeling, and air pollution dispersion. Measurements of NO_2 were conducted mid-block along four segments of the corridor throughout a 4-week campaign conducted between March and April 2015. The four segments were chosen to be consecutive and yet exhibiting variability in road configuration and built environment characteristics. Roadside NO_2 measurements were also paired with on-site meteorological data collected using a portable meteorological station. In addition, traffic volumes, composition, and routing decisions were collected using video-cameras located at upstream and downstream intersections. Dispersion of simulated emissions was calculated for 8 time slots and under a range of meteorological conditions using three different models (OSPM, CALINE4, and SIRANE) with vastly different dispersion algorithms. While OSPM and SIRANE led to simulated concentrations having a better match against measured concentrations on road segments with buildings on both sides, CALINE4 led to a better match with measured data when the built environment mostly involves open terrain. All three models revealed a better performance when wind speed was higher than 1.5 m/s. The performances of OSPM and CALINE4 were also constrained by wind direction, while SIRANE overcame this shortcoming. In conclusion, SIRANE exhibited better overall performance compared to the other two dispersion models.

Keywords: traffic simulation; emission modeling; dispersion modeling; OSPM; CALINE4; SIRANE; MOVES; nitrogen dioxide; Montreal; urban canyon; near-road air pollution

RÉSUMÉ

La pollution atmosphérique liée aux transports est associée à des effets indésirables sur la santé dans les milieux urbains. Ces effets néfastes sont plus prononcés à cause de la circulation routière qui est un produit des quartiers résidentiels et commerciaux à haute densité, ainsi que les effets du cadre bâti qui peuvent exacerber les symptômes des maladies respiratoires. Puisque les risques de l'exposition prolongée aux polluants atmosphériques sont plus élevés dans les régions urbaines, il est donc nécessaire de mieux comprendre les effets de la dispersion atmosphérique et de la recirculation de l'air et également d'identifier les méthodologies afin de les reproduire.

Le but de cette dissertation s'agit de deux composants principaux. Le premier but concerne l'intégration de la simulation microscopique de la circulation routière, le calcul des émissions et la modélisation de la dispersion atmosphérique qui peuvent reproduire la recirculation de la pollution de l'air dans les environnements urbains. Le deuxième objectif examine l'estimation, la validation et la comparaison des modèles qui peuvent ensuite déterminer le modèle optimal selon la forme du cadre bâti.

Afin d'accomplir ces objectifs, les concentrations du dioxyde d'azote (NO_2) mesurées au bord de la rue, un marqueur de la pollution de l'air liée à la circulation, ont été simulé au bord d'une artère importante située à Montréal, Québec en utilisant des méthodes de simulation microscopique de la circulation, modélisation d'émissions instantanées, et la dispersion de la pollution atmosphérique. Les mesures NO_2 ont été exécutées sur quatre segments de la rue pour quatre semaines pendant les mois de mars et d'avril 2015. Les points de mesure ont été choisis pour refléter les différences des caractéristiques portant sur l'orientation de la voie de la circulation et du cadre bâti. Les mesures NO_2 ont été couplées avec les données météorologiques mesurées sur place par une station météo portable.

Ensuite, les volumes de la circulation routière, leur composition, ainsi que les décisions routières ont été accueillies en utilisant des caméras vidéos situés en amont et en aval des carrefours. L'effet de la dispersion des émissions simulées a été effectué pour huit périodes temporales qui démontrent une variété des conditions météorologiques en utilisant trois modèles différents (OSPM, CALINE4, et SIRANE).

Tandis que l'utilisation d'OSPM et SIRANE a mené à des concentrations simulées qui sont plus similaires avec les concentrations mesurées lorsque le point de mesure est situé dans un canyon urbain, les résultats de CALINE4 a été plus compatible avec les données réelles où les espaces ouverts sont impliqués. En plus, quand la vitesse du vent a été plus forte que 1.5 m/s, les performances des modèles ont amélioré. L’efficacité de l’OSPM et CALINE4 a été affectée négativement par la direction du vent, tandis que ce paramètre a compté un effet neutre en utilisant SIRANE. En conclusion, SIRANE a démontré les meilleurs résultats parmi les trois modèles.

Mots-clés : simulation de la circulation routière, modélisation des émissions, modélisation de la dispersion atmosphérique, OSPM, CALINE4, SIRANE, MOVES, dioxyde d’azote, Montréal, canyon urbain, pollution atmosphérique à l’échelle de la rue

LIST OF FIGURES

Figure 1.1: Methodological Flow Chart of the Thesis 4

Figure 3.1: Study Site 17

Figure 3.2: A Snapshot of Aeroqual S500 Sensor Software 19

Figure 3.3: Captured Traffic Information by Digital Camcorder 20

Figure 3.4: Set-up Equipment for the Field Data Collection Campaign 22

Figure 3.5: Location and Monitoring Station Molson (Source: RSQA) 24

Figure 4.1: Definition of Street Orientation 31

Figure 4.2: Wind Profiles during the Campaign in Each Time Period at McTavish Station 33

Figure 4.3: Histogram of Corrected NO_2 Concentrations 36

Figure 4.4: Fixed-station and Roadside Measured NO_2 Concentrations Paired in Time 37

Figure 4.5: Box Plot Comparison between Fixed and In-situ Measurements 38

Figure 5.1: VISSIM Traffic Simulation Network 42

Figure 6.1: Sketch of a Typical Street Canyon 47

Figure 7.1: Comparison between Simulated and Observed Traffic Volumes at Segment 1 (a), Segment 2 and 3 (b), and Segment 4 (c) 57

Figure 7.2: Box Plot of Simulated Results 60

Figure 7.3: Scatter Plot of Simulated vs. Measured Concentrations 63

LIST OF TABLES

Table 2.1: Adverse Health Effects of NO_2 & PM ((World Health Organization 2013))..........7

Table 3.1: Field Work Locations on Ave. Papineau..16

Table 3.2: Specifications of the Aeroqual Sensors (source: Aeroqual Inc.)............................18

Table 3.3: Random Time and Location Schedule...21

Table 3.4: GIS Data Resources Table..25

Table 4.1: MOVES2010b On-road Source Types (source: US EPA) 28

Table 4.2: Descriptive Statistics for Hourly Traffic 29

Table 4.3: Descriptive Statistics for Meteorological Data..31

Table 5.1: Street Configuration Parameters (in the order from northwest to southeast).........41

Table 6.1: Pasquill Stability Class Paired with Wind Direction Standard Deviation.............50

Table 6.2: Summary of Performance Measures for Dispersion Model Validation 53

Table 7.1: Emission Factors with Respect to 8 Time Slots and 4 Road Segments.................58

Table 7.2: Validation against Roadside Measurements..62

Table 7.3: Validation against Fixed-station Data 62

Table 7.4: Comparison between Different Wind Speeds..65

Table 7.5: Comparison between Wind Directions..66

LIST OF ABBREVIATIONS

NO_2	Nitrogen Dioxide
NO_x	Nitrogen Oxides
US EPA	United States Environmental Protection Agency
WHO	World Health Organization
RSQA	Réseau de Surveillance de la Qualité
NAPS	National Air Pollution Surveillance
LUR	Land Use Regression
VISSIM	Verkehr In Städten- SIMulationsmodell
MOVES	Motor Vehicle Emission Simulator
OSPM	Operational Street Pollution Model
CALINE	CAlifornia LINE source model
FB	Fractional Bias
NMSE	Normalized Mean Square Error
NAD	Normalized Absolute Difference
FAC2	Fraction within 0.5 and 2
MG	Geometric Mean Bias
VG	Geometric Mean Variance

ACKNOWLEDGEMENTS

First of all, I would like to devote my most sincere gratitude to my supervisor, Professor Marianne Hatzopoulou, for her remarkable support, invaluable guidance and consistent patience, which encourage me to pursue higher goals throughout my studies at McGill University. Her knowledge, enthusiasm, dedication, and deep insight to transportation research have been inspiring and benefiting me through my research career. I am also grateful that McGill University and the Civil Engineering Department can accept me, provide me with world-class platform and make the entire dream true.

I would also like to express my deep gratitude to my friends and teammates in our study group, without whom I can never finish such a complicated and arduous research project: Junshi Xu, Yulin Hu, and Alexander Lee. I also feel lucky and thankful that I have met a lot of young fellows that share the same interest in transportation research as I do: Dr. Ahsan Alam, Maryam Sherkarrizfard, Dr. Masoud Fallahshorshani, Miguel Domiguez Michelen, Laura Minet, Laure Deville Cavellin, Kenan Al Rijleh and Muhammad Yousuf Khan. Thanks to them, my college time in Montreal has become more vivid and more unforgettable than ever. In addition, I would like to thank my friend either in the same major or elsewhere in the McGill Community: Ting Fu, Jinhui Ding, Tianlu Liu, Gaowei Xu from Civil Engineering department, Professor Ahmed El-Geneidy, Dr. Ehab Diab from School of Urban Planning.

Ultimately, I am so grateful that my parents, Shaohui Wang and Min Ding, have been supporting me financially and mentally throughout my two-year master studies at McGill University. I feel indebted to their consistent trust and backup.

PREFACE AND CONTRIBUTION OF AUTHORS

This thesis presents an arduous, yet meaningful and marvelous field measurement campaign conducted during the harsh winter months to analyze near-road air pollution. This study thus has a firm foundation based countless hard-working days and nights.

Firstly, I would like to mention the remarkable efforts of the teammates in our data collection group. Junshi Xu, Yulin Hu, and Alexander Lee have spent an enormous amount of time on the data collection and processing campaign, which largely facilitated further analysis. Without them, the study presented in the thesis can never be finished in such a neat and efficient way. In particular, I sincerely appreciate Junshi Xu for his help in helping me sorting out collected data, and constructing the traffic simulation network. Furthermore, I would like to thank Alexander Lee, as well as Shiyu Wang, for their kind and patient work writing up the French abstract and helping me improve my thesis' write-up and structure. In addition, it is very worth mentioning that Dr. Masoud Fallahshorshani has done extensive contribution towards operating and running SIRANE model. Professor Ronald Gehr also has provided valuable and very helpful opinions and advice for my thesis.

Last but not least, I would like to mention the most remarkable and indispensable contribution from my supervisor, Professor Marianne Hatzopoulou, without whom I will never have the chance to enter such an intriguing research. All of these materials related to this thesis were prepared collaboratively with her. Her invaluable guidance and firm support is the motivation that leads me to today's position.

CHAPTER 1 INTRODUCTION

1.1 Background and Motivation

Traffic-related emissions play a dominant role in urban air pollutant concentration levels despite great improvements made in combustion engine technology and are associated with a number of chronic and acute health effects (Vardoulakis et al. 2003). For example, exposure to nitrogen dioxide (NO_2) has been positively associated with increased airway responsiveness in asthmatic individuals after short-term exposures and respiratory illnesses in children with longer-term exposures (United States Environmental Protection Agency 2008). Other studies also found a positive correlation between NO_2 and incidences of breast cancer, heart attacks and asthma (Crouse et al. 2010; Parent et al. 2013; Wu et al. 2011).

In order to control and monitor ambient air pollution, significant materials and human resources have been invested into establishing a nation-wide air quality monitoring system in Canada. Since 1969, the National Air Pollution Surveillance (NAPS) system was founded to monitor and assess ambient air pollution including sulfur dioxide (SO_2), Particulate Matter (PM), Nitrogen Oxides (NO_x) in populated regions of Canada (Environment Canada 2013). For the city of Montreal, the 'Réseau de surveillance de la qualité de l'air' (RSQA) runs 13 monitoring stations providing daily air quality assessment. However, fixed-station monitoring on its own is not sufficient to capture the characteristics of instant chemical processes and prompt air pollutant concentrations caused by local vehicular sources, often, researchers rely on portable air pollution monitors and sensors to characterize near-road air pollution (Weichenthal et al. 2014; Mead et al. 2013).

Along with fixed-station and *in-situ* air quality monitoring, studies on dispersion modeling have been well developed. Unlike field measurements, dispersion modeling is more cost-efficient, allowing for shorter sampling periods and less resource investment. It can be conducted on different spatial and temporal scales that field measurements may not be able to capture. Furthermore, dispersion modeling is extremely useful in testing future projects, plans and regulations and assessing their feasibility. In other words, dispersion modeling can make predictions while field measurements cannot. Thus, a vast amount of dispersion models were developed fitting different utilities. Among them, a dispersion model called 'street canyon' was proposed especially to tackle traffic emission dispersion in urban built environments. This model represents the presence of buildings flanking both sides of the street, and whose configuration may cause recirculation and dispersion patterns different than what may be observed in other urban settings. (Kakosimos et al. 2010). This phenomenon, known as the 'street canyon effect', is extremely prevalent in urban areas and consequently, numerous theories and software have been developed by academic researchers to better understand and explain this effect. In order to improve the methods used to study the dispersion of air pollutants in street canyons, it is necessary to validate dispersion model output against *in-situ* and fixed-station data under the same evaluation criteria.

This thesis presents the experimental design and results of a four-week data collection campaign, dispersion modeling using three different models (OSPM, CALINE4 and SIRANE), along with the validation and comparison between the three models. This study aims to understand traffic-related air pollutant dispersion in near-road environments concerning unique dispersion patterns caused by the street canyon effect and to assess the suitability of related software and methodologies. It is useful for planners in the design of complete streets and active transportation facilities aimed to minimize individual exposure, and for air pollution researchers to better understand the advantages and disadvantages of each model depending on its context.

1.2 Objectives

This thesis has two main objectives:

1) To develop an integrated model chain combining traffic simulation, emission modeling, and dispersion modeling.
2) To determine and evaluate the performance of three dispersion models and validate their usage by comparing with field measurement and fixed-station data.

1.3 Summary

A literature review follows this chapter tackling several topics including air pollution and health, dispersion modeling, and comparison between dispersion models. The association between adverse health effects and traffic-related air pollution, mainly traffic-related NO_2, has been highlighted, which motivates the research in this thesis. This is followed by a review of academic studies on dispersion modeling, as various dispersion modeling methodologies have been developed. Finally, a comparison between dispersion models is presented.

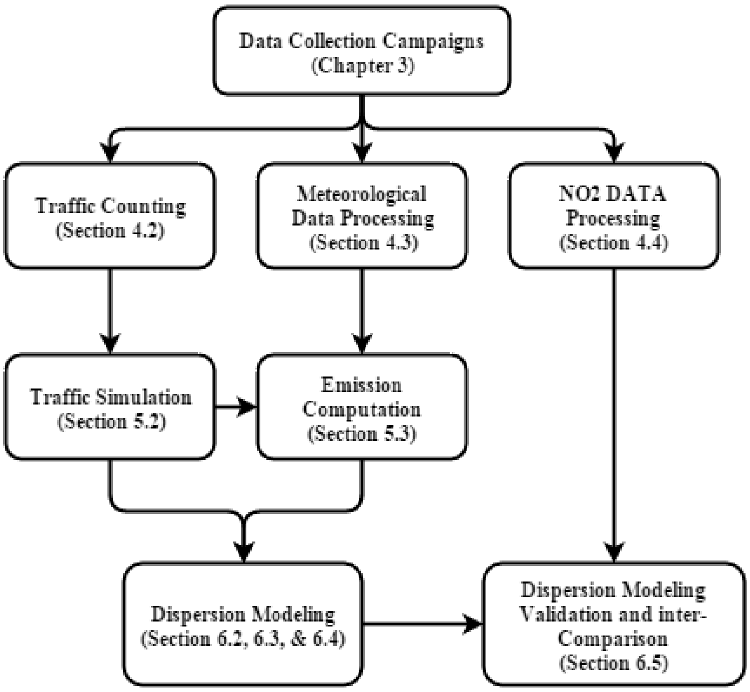

Figure 1.1: Methodological Flow Chart of the Thesis

Chapter 3 presents the data collection campaign consisting of two major components: the field measurement campaign conducted onsite and the fixed-station data collection campaign. Figure 1.1 illustrates how data collection campaigns play integrated roles in the methodology presented in this thesis.

Chapter 4 outlines the processing of meteorological data from *in-situ* measurements and fixed stations, the traffic counting process and protocol, and *in-situ* measured and fixed-station NO_2 concentrations.

Chapter 5 focuses on the processing of traffic simulation and emission estimation. This chapter translates real-world primary data into a format that can be employed directly as inputs for dispersion models.

Chapter 6 outlines the algorithms of three dispersion models of interest, namely, the OSPM model, CALINE4 model, and the SIRANE model. The final products of our dispersion modeling chain, link level NO_2 concentrations, are also presented in this chapter.

Chapter 7 presents the results of model validation using a set of performance indicators available in the literature. .

Chapter 8 discusses and summarizes the results and findings discovered throughout the thesis. Limitations and future work were also put forward at the end of this chapter.

CHAPTER 2 INTEGRATION OF TRAFFIC SIMULATION, EMISSION ESTIMATION AND DISPERSION MODELING: STATE OF THE ART AND PRACTICE

2.1 Introduction

Traffic related air pollution has contributed to serious health problems and for this reason has been thoroughly studied. An emerging topic in this field is the development of modeling chains whereby traffic simulation, emission estimation, and dispersion modeling are conducted. This chapter begins by exploring the adverse health effects associated with traffic-related air pollution in Section 2.2. Then follows with the research studies that explore the generation and dispersion of traffic-induced air pollution in Section 2.3. Finally, Section 2.4 reviews validation methods and specifically the inter-comparison of several commonly used dispersion models.

2.2 Traffic-Related Air Pollution and Health

Short-term exposure and long-term exposure to air pollution at different levels have been associated with various adverse effects on human health. The World Health Organization has summarized a series of adverse health effects associated with short-term and long-term exposure to air pollution in Table 2.1. Due to the scale of this study, only NO_2 and particulate matter will be emphasized.

Table 2.1: Adverse Health Effects of NO_2 & PM ((World Health Organization 2013))

Short-term exposure effects
Daily mortality
Respiratory and cardiovascular hospital admissions, emergency department visits and medication uses
Acute symptoms (wheezing, coughing, phlegm production and respiratory infection)
Physiological changes (e.g. lung function)
Long-term exposure effects
Mortality due to cardiovascular and respiratory disease
Chronic respiratory disease incidence and prevalence
Chronic changes in physiological functions
Lung cancer
Chronic cardiovascular disease
Intrauterine growth restriction (low birth weight at term, intrauterine growth retardation, small for gestational age)

Among the family of highly reactive NOx, NO_2 is the primary pollutant of interest in the urban air pollution context, with transportation activities representing the main source of urban NO_2 emissions (Felix and Elliott 2014). The US Environmental Protection Agency (EPA) suggests that short-term exposure to NO_2 may lead to adverse respiratory effects in healthy people and increased respiratory symptoms in people suffering from asthma (United States Environmental Protection Agency 2008). A number of epidemiological studies indicate that traffic-related NO_2 has been associated with the increased risk of postmenopausal breast cancer, prostate cancer and other adverse reproductive outcomes (Crouse et al. 2010; Parent et al. 2013; Wu et al. 2011). Cohort studies have also found that NO_2 was associated with life-time history of asthma and wheezing, with a positive correlation between residential location and its distance to a highway (Brauer et al. 2007). This finding is especially important for households with children, as childhood exposure to NO_2 may lead to deficits in the growth of lung function between the ages of 10 to 18 (Gauderman et al. 2005).

While there exists a plethora of academic literature examining the health impacts of one pollutant on its own, few studies have covered those of multiple air pollutants in proximity to roads. Such studies mainly focused on NO_2 and particulate matters, which are deemed as important indicators of traffic emissions. They were significantly associated with higher blood cholesterol, respiratory mortality and infections, and asthma for children under 4 (Sørensen et al. 2015; Beelen et al. 2007). However, the results suggested difficulty in explaining the interaction between these two pollutants. In addition, other studies also examined the effects of traffic-related air pollution and noise simultaneously. However, the role played by noise in the study was only slightly associated with cases of disease. Despite this finding, the author noted the difficulty in distinguishing an association between noise and air pollution was difficult to separate (Sørensen et al. 2015).

With all the adverse health effects being presented, the purpose of this literature review is to emphasize the necessity of further air pollution studies. In high-density urban environments where construction activities and traffic congestion are common, it is essential to understand how traffic-induced air pollution can affect public health and to understand the emission and dispersion pattern of urban air pollution in order to improve the urban design components which will mitigate these effects.

2.3 Air Pollution Dispersion Modeling

In urban areas, air pollution is affected by factors relating to the built environment, traffic composition and meteorological conditions. In order to capture the spatial distribution of NO_2 in urban areas, land use regression (LUR) models have been widely used to generate NO_2 surfaces (Kim and Guldmann 2015; Liu et al. 2015; Shekarrizfard et al. 2015), which can also be combined with home location or mobility data to evaluate exposure in epidemiological studies (Crouse et al. 2010; Parent et al. 2013). With the application of advanced geographic information system (GIS), high-resolution air pollution distribution maps can be generated with higher efficiency. However, it is difficult to understand real-time air pollutant dispersion or chemical processes using LUR models on a smaller spatial scale (Knibbs et al. 2014; Kerckhoffs et al. 2015). Also LUR models need prolonged sampling periods to average through extreme concentrations and meteorological changes. Since a difference exists between roadside and non-roadside air pollution concentrations (Weichenthal et al. 2014; Baldwin et al. 2015) . As a result of distance-decay gradients, it is necessary to study prompt traffic emissions and dispersion.

Emission and dispersion models are often used to investigate the effects of near-road air pollution concentrations for their cost-efficiency and ability to reproduce air pollution dispersion. Near-road dispersion studies often focus on heavy traffic links of a major corridor (Kenty et al. 2007; Zhang and Batterman 2013; Murena et al. 2009; Karim and Nolan 2011) or small road networks (Wallace and Kanaroglou 2008) These studies consist of three main steps: traffic estimation, emission modeling, and dispersion modeling. Traffic estimation can either be done by on-site traffic counting (Benson 1992; Kenty et al. 2007; Levitin et al. 2005), or derived from travel demand data and traffic simulation (Wallace and Kanaroglou 2008; Amirjamshidi et al. 2013; Hatzopoulou and Miller 2010). Emissions are often estimated using average link speeds (Wallace and Kanaroglou 2008; Kenty et al. 2007; Levitin et al. 2005; Hatzopoulou and Miller 2010) or real-time link drive-cycles (Amirjamshidi et al. 2013). Various dispersion models were utilized in these studies combined with traffic estimation and emission calculation to understand air pollution dispersion patterns at different spatial levels. In meso- and macro-simulations, travel demand assignment and travel behavior prediction along with average speed emission calculation are often integrated with dispersion models yielding comprehensive insight on air pollution dispersion within road networks (Hatzopoulou and Miller 2010; Hülsmann, Gerike, and Ketzel 2014; Berrone et al. 2012). Furthermore, on-site traffic counting and real-time traffic simulation are always paired in link-level dispersion modeling (Amirjamshidi et al. 2013; Kukkonen et al. 2001) which allows for more detailed information on air pollution levels within roadside environments.

There are currently many models and methodologies that have been designed and developed to accommodate different pragmatic and academic projects in various urban environments. Therefore it is imperative to avoid misuse of dispersion models which would lead to inappropriate conclusions. Thus the process of choosing and validating different models while considering the context in which the model would be employed also became a notable topic in current academic discourse.

2.4 Validations and Comparison between Dispersion Models

In order to evaluate and validate different types of dispersion models, several air quality model performance measures were proposed by Chang and Hanna (2004), including fractional bias (FB), normalized mean square error (NMSE), normalized absolute difference (NAD), etc. Furthermore, Hanna and Chang (2012) put forward several location-specific criteria for the performance measures to consider rural air dispersion models and urban air dispersion models. These measures and criteria were widely accepted and applied into several other studies to evaluate and validate the performance of air dispersion models (Soulhac et al. 2012; Carpentieri et al. 2012; Jensen et al. 2009; Rood 2014).

To evaluate and validate the performance of dispersion models, experimental measurements are required to utilize these criteria. There are several ways to obtain measured air pollution data. For newly developed models, wind tunnel experiments can be efficient to gather information under case control conditions. In this manner, the behavior and reaction of dispersion models to a specific impact factor such as wind direction can be systematically detected (Carpentieri et al. 2012). Moreover, measured data can be obtained from fixed air quality monitoring stations in the study area. This method is often employed in land use regression model evaluations as well as projects of large spatial scale. While data from fixed stations is relatively easy to obtain, the fixed-station data cannot describe near-road air pollution patterns and prompt air pollutant concentration changes. Another common data collection method is to measure on-site using portable air quality sensors. While it consumes much material and human resources to accomplish, with proper experiment design, it overcomes the shortcomings of using data from fixed stations.

There are currently several well-established and validated dispersion models widely used in academia and in real-world practice: Operational Street Pollution Model (OSPM) which has been designed and widely used in Europe to study traffic pollution for 20 years; CAlifornia LINE source model 4 (CALINE4), widely used in the USA, published in 1984 as the latest successor of CALINE dispersion modeling software family, and SIRANE, newly developed model in Lyon, France, 2011, with satisfying performance against field measurements. They have been tested against wind tunnel experiments, fixed-station and field measurements in numerous studies (Carpentieri et al. 2012; Kukkonen et al. 2001; Ghafghazi 2014). Three main considerations determined the selection of dispersion models. First of all, the three models all have great popularity in both Europe and the US, yet they have not been used or validated extensively in the Canadian context. Secondly, the purpose of this thesis is to examine air pollution dispersion in near-road environments (rather than at a regional level), which is exactly what the three models are intended to be used for. Finally, the three models demonstrate the history of dispersion model development ranging from a simple Gaussian model (CALINE4) to the combination of box model and Gaussian model (OSPM), and finally the addition of inter-exchange airflow at intersections (SIRANE). Nevertheless, to select a suitable dispersion model for different applications, there is another important procedure, which is to compare several sets of dispersion models under different urban conditions. The comparison between models is based on the application of the aforementioned evaluation measures and criteria (Beelen et al. 2010; C. Mensink et al. 2006). The most commonly used dispersion models to date apply the Gaussian line source dispersion model as the core algorithm, including CALINE4 and OSPM. These dispersion models suffer in that they are affected by the most prominent shortcoming of the Gaussian model (Holmes and Morawska 2006), which is known to exhibit poor performance under the conditions of low wind speeds (<1.5 m/s) and parallel wind directions (difference between the angle of wind direction and the angle of the roadway smaller than 10 degrees). SIRANE, as a newly developed model, does not completely apply Gaussian line sources. Thus, though it still behaved poorly at low wind speeds, the SIRANE exhibits acceptable performance when the wind blows parallel to the roadway (Soulhac et al. 2012).

2.5 Contributions

This thesis includes several contributions to the research field of near-road air pollution dispersion. First, the research sheds light on those road configurations and meteorological conditions that are most and least prone to the dispersion of traffic-related air pollutants. Second, it proposes and validates an integrated dispersion modeling chain to simulate roadside NO_2 dispersion. Finally, this study enriches the literature on air pollution research in terms of the performance of dispersion models under various land-uses and road geometries. Their performance was validated and compared in terms of their compliance with a set of unified evaluation criteria.

2.6 Conclusion

As the adverse health effects caused by traffic-related air pollution are exacerbated in urban settings, it is paramount to improve current practices aimed at curtailing concentration levels. As two cornerstones of air pollution research, solutions are required to better integrate air quality monitoring and dispersion modeling in research and to deepen our understanding of their interaction with one another.

This thesis aims to systematically validate, evaluate and compare three commonly used urban air pollution dispersion models, OSPM, CALINE4 and SIRANE, with on-site measured NO_2 data and data extracted from fixed stations. Thus, a measurement campaign were carried out in the months of March and April of 2015, along Papineau Avenue, which was a significant high-volume street in Montreal, Canada. Differences in this study's methodology compared to related studies can be summarized as follows:

1) Field measurements were carried out in several selected study sites exhibiting differences in built environments illustrated in the following chapter. It is important to note that traffic characteristics and meteorological conditions were consistent for all study sites. This eliminated several obstacles in the form of differences in traffic composition and weather, facilitating the performance assessment of dispersion models.
2) Traffic simulation was based on real-world traffic counting data. Emission estimation was derived from second-by-second simulated traffic conditions. Thus, accurate traffic and emission data were input into dispersion models.
3) Comparison between three commonly used dispersion models was conducted under different meteorological and land use conditions. This could be very helpful for regulatory and academic projects to determine which dispersion model suits which case.

CHAPTER 3 DATA COLLECTION METHODOLOGY

3.1 Introduction

The on-site measurement campaign was designed and prepared in January 2015. *In-situ* measurements and fixed-station data collection campaigns were conducted in March and April of 2015. *In-situ* measurements were carried out along Papineau Avenue in Montreal, Canada. The fixed-station data collection took place in the same time period. Fixed-station meteorological data and ambient pollutant levels were extracted from nearby weather and air monitoring stations. Section 3.2 focuses on the *in-situ* data collection. The instruments used during the campaign are described in Section 3.2.2 and the protocol of the data collection campaign is shown in Section 3.2.3. Section 3.3 describes the data collected from fixed stations.

3.2 *In-situ* Data Collection

3.2.1 Corridor Selection

Due to the lack of a near-road air pollution monitoring network in the city of Montreal, the roadside air pollution data used in the thesis were collected on-site using portable air pollution sensors. Air quality data were collected at four different sites varying in built environment characteristics along Papineau Avenue in Montreal. Both ends of this avenue lead to bridges connecting the City of Montreal with the rest of the region, making it a high-volume road servicing local and “through” traffic. Each of the four data collection sites is located mid-block along a segment of Papineau Avenue. The detailed locations of air quality and traffic monitoring sites are presented in Table 3.1.

Table 3.1: Field Work Locations on Ave. Papineau

No.	Location Address	Intersection Code	Corresponding Intersection
1	4265 Avenue Papineau	A	Ave. Papineau/Rue Marie-Anne
2	4065 Avenue Papineau	B	Ave. Papineau/Rue Rachel
3	3535 Avenue Papineau	B	Ave. Papineau/Rue Rachel
4	2175 Avenue Papineau	C	Ave. Papineau/Rue Sherbrooke

Figure 3.1 illustrates the four different segments (1 to 4) and surrounding environment. Segment 1 is predominantly surrounded on both sides by low residential buildings, with an average height of 9.7 meters. Segment 2 has low residential buildings one side of the road and a park (Parc La Fontaine) located on the opposite side. Segment 3 is bound by high residential buildings on one side (with an average height of 20 m) and park area on the other. The last segment has a gradient of -4.29% in the southbound direction, with low commercial and residential buildings on both sides of the street. The four segments were selected in an effort to maximize variations in the set of potential built environment predictors of NO_2, while maintaining relative consistency in terms of traffic volume and composition.

Map of Montreal Island (Study Site Higlighted in Red)

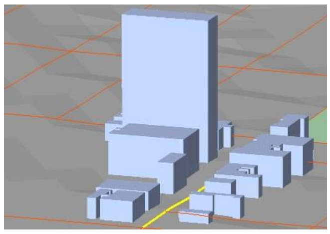

Segment 1

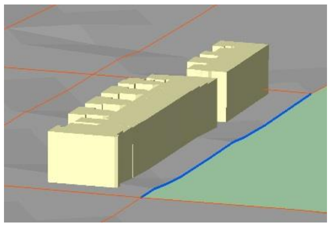

Segment 2

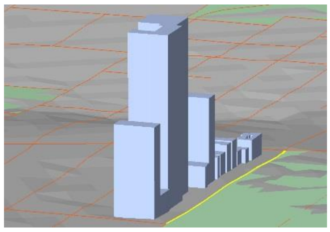

Segment 3

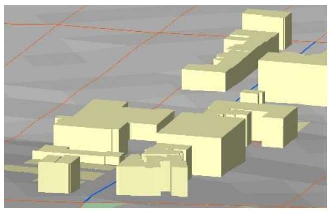

Segment 4

Figure 3.1: Study Site

3.2.2 Instruments

3.2.2.1 Aeroqual S500 Sensor

The near-road NO_2 concentrations were collected using Areoqual S500, a portable air quality sensor manufactured by Aeroqual Ltd. New Zealand. Detailed specification can be found in Table 3.2. The technology for O_3 is the Gas Sensitive Semi-Conductor (GSS), Aeroqual. The technology for NO_2 is the Gas Sensitive Electrochemical technology. For both sensors, an internal fan pulls air across the gas sensor every 60 seconds, resulting in a minimum response time of 60 seconds. The long-life lithium battery allows trips of more than 8 hours without need for recharge. The data can be converted into .csv format thanks to software provided by Aeroqual, as shown in Figure 3.2.

Table 3.2: Specifications of the Aeroqual Sensors (source: Aeroqual Inc.)

	Gas Sensor	Range (ppm)	Minimum Detection Limit (ppm)	Accuracy of calibration	Resolution (ppm)	Operational range	
						Temp.	RH
	O_3	0-0.5	0.001	<±0.008 ppm 0-0.1 ppm; <±10% 0.1-0.5 ppm	0.001	0 to 40°C	10 to 90%
	NO_2	0-1	0.005	<±0.02 ppm 0-0.2 ppm; <±10% 0.2-1 ppm	0.001	0 to 40°C	10 to 90%

Two Aeroqual sensors were utilized in the *in-situ* data collection campaign, one for NO_2 and another for O_3.They were positioned together horizontally 1.2 m above the ground and as close as possible to the curb. The receptor positions in the dispersion models were also placed at the same altitude accordingly. NO_2 and ozone (O_3) concentrations were collected and recorded simultaneously every minute for 2 hours. The reason for co-locating an O_3 sensor with the NO_2 sensor is due to the NO_2 sensor's cross-sensitivity to O_3. While the O_3 sensor only measures O_3, the NO_2 sensor detects both NO_2 and O_3 and therefore the O_3 concentration should be subtracted from the NO_2 reading.

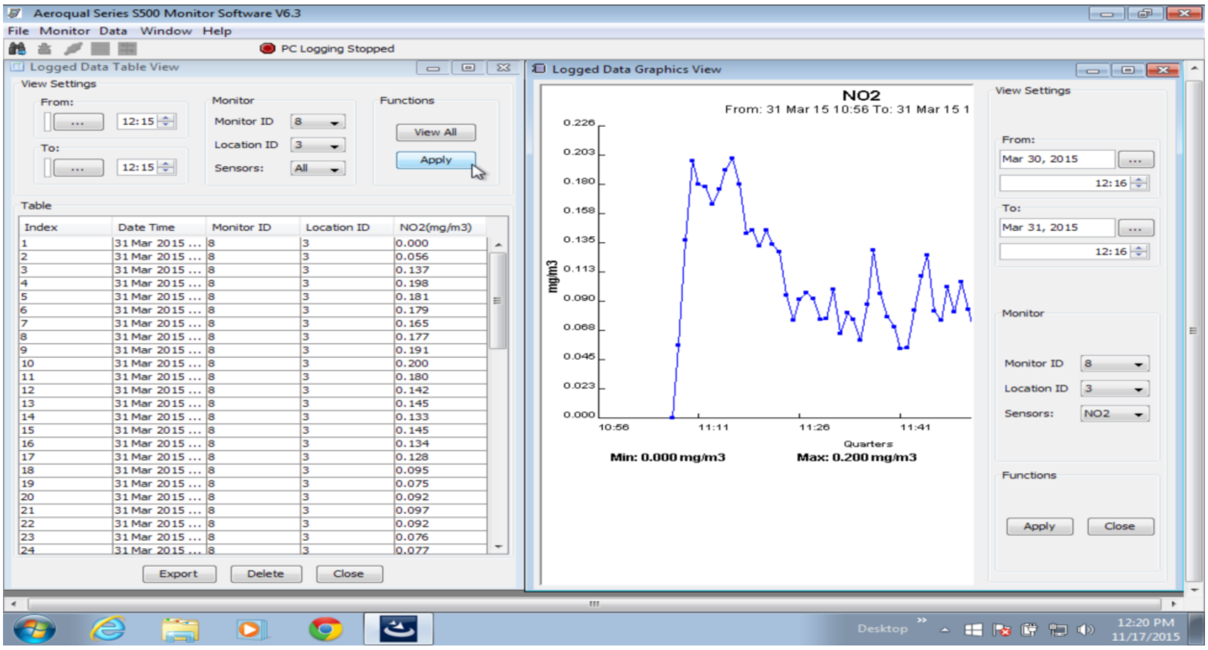

Figure 3.2: A Snapshot of Aeroqual S500 Sensor Software

3.2.2.2 Portable Weather Station

An ambient weather WS-2095 (Ambient Weather, Chandler, AZ, USA) wireless portable weather station was used for measuring meteorological data such as temperature and humidity at specifically selected points along Papineau Avenue. We collected these data to describe more accurate meteorological conditions on site.

Measurements at 15-minute intervals were selected. The station was positioned on the same side of the road with NO_2 and O_3 sensors, in order to provide exact on-site weather conditions, and all weather history data recorded by the base station were uploaded to a manufacturer's software, Easyweather. The data was then exported in CSV files.

3.2.2.3 Digital Camcorder

The traffic flow data were recorded by two commercially available video camcorders (Hero 2, Hero 3 GoPro, GoPro Inc., San Mateo, CA, USA) mounted on top of the traffic light controller box on each intersection during the data collection campaign. With a 170 degrees wide-angle view, the cameras were able to provide detailed information of vehicle types as well as vehicle routing decisions, as shown in Figure 3.4. The cameras recorded high-resolution video (720p) at 60 frames per second.

Figure 3.3: Captured Traffic Information by Digital Camcorder

3.2.3 Data Collection Protocol

Field data measurements were conducted on 16 weekdays over a four-week period in the months of March and April of 2015. To avoid selection bias, visits to the measurement locations were randomly scheduled to be conducted four days per week on the principle that each abovementioned segment (Section 3.2.1) would be measured once in one time period each day as shown in Table 3.3. Data collection was conducted during peak morning (08:00 -10:00) and afternoon (16:00 - 18:00), as well as off peak in the mid-day (10:30 -12:30) and (13:30 - 15:30).

Table 3.3: Random Time and Location Schedule

Week 1	Mo.	Tu.	We.	Th.	Fr.	Week 2	Mo.	Tu.	We.	Th.	Fr.
8:00-10:00		2B	4C	1A	4C	8:00-10:00	3A		4C	2B	1B
10:30-12:30		1A	2B	4C	1A	10:30-12:30	4C		1A	1B	3B
13:30-15:30		3B	1A	2B	3C	13:30-15:30	2A		3B	4C	4C
16:00-18:00		4C	3C	3B	2B	16:00-18:00	1A		2B	3C	2B
Week 3	Mo.	Tu.	We.	Th.	Fr.	Week 4	Mo.	Tu.	We.	Th.	Fr.
8:00-10:00	3B	2B		1A	3B	8:00-10:00	2B	1A		4C	3B
10:30-12:30	4C	3B		4C	2B	10:30-12:30	3B	3B		2B	2B
13:30-15:30	1A	4C		2B	1A	13:30-15:30	4C	2B		3C	1A
16:00-18:00	2B	1A		3B	4C	16:00-18:00	1A	4C		1A	4C

Note: Numbers and letters are corresponding to Table 3.1.

At the same time, meteorology data was logged and averaged at 15-minute intervals by the wireless weather station. Weather data were recorded at an altitude of approximately 1.5 meter, and the console of the weather station was placed beside for monitoring the working condition of weather situation through wireless communication. All air quality instruments as well as the portable weather station were placed in the middle of each particular segment, in case recorded concentrations were greatly influenced by the pollutants produced by traffic on the cross roads.

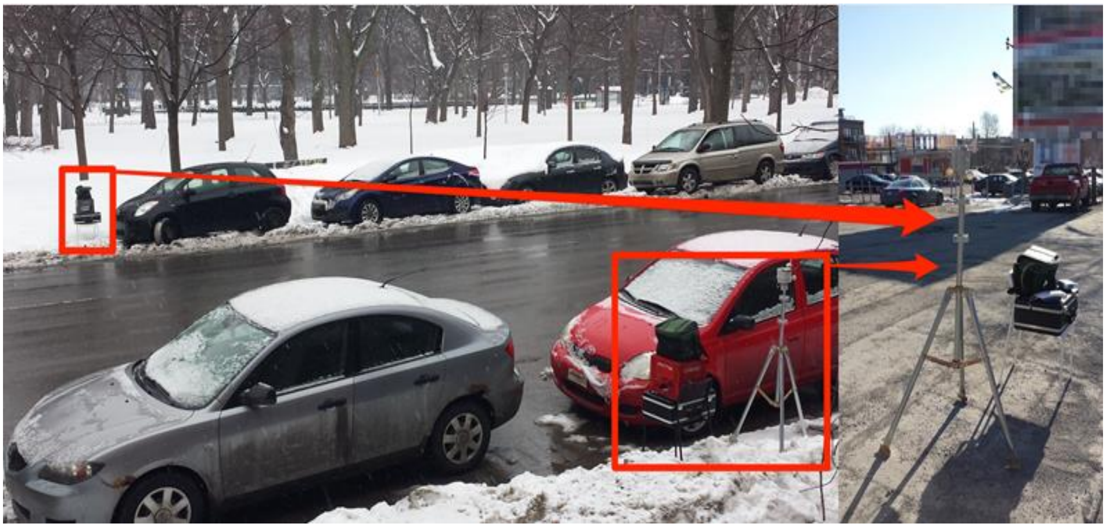

Figure 3.4: Set-up Equipment for the Field Data Collection Campaign

At the same time, the digital camcorder was affixed on the traffic light controller box located at the upstream intersection corresponding to measured road segments, recording real-time traffic information, including vehicle type, vehicle counts for all directions and their corresponding route decisions.

All instruments' clocks were synchronized daily and examinations of proper operation were carried out every 30 min. In the event of malfunction, specific instruments were restarted and calibrated when possible. Visual observation of local traffic conditions, abnormally high concentration readings, and prominent non-vehicular emissions (e.g., roadside construction sites) were manually recorded.

In total, sampling time at each location lasted 2 hours, and approximately 8 hours were required for one complete set of measurements at each location. Upon the completion of each day of field measurements, all real-time NO_2, weather data and video data of traffic were downloaded, inspected, and archived immediately in an external hard drive. All NO_2 measurement files were saved with a standardized naming convention, which included location

ID, instrument ID, year, month, day, time period, and data type. Potential data quality issues involving missing data, negative or otherwise spurious readings were flagged for subsequent evaluation and analysis.

3.3 Fixed-station Data Collection

3.3.1 Meteorological Data

The meteorological data used in this thesis came from two sources. The first source is the portable weather station on site, while the second source being the McTavish weather station in Montreal. The MacTavish station is located on the McGill University downtown campus, approximately 4 km from the study location. Meteorological data can be downloaded from its website in .csv format, with the default time interval of 1 hour.

Theoretically, we should also measure the wind profile at the study site to better synchronize with other measured data. However, the dispersion model procedure required wind profile at rooftop level in order to simulate how it penetrates the urban canyon. Also, the wind profile in the built environment where we conducted our measurements was severely impacted by traffic-induced and street canyon vortices and eddies. Thus, fixed-station meteorological data could be a very useful supplement to our study.

3.3.2 NO_2 Concentrations

In this study, the simulated results were compared with both *in-situ* measured NO_2 concentrations as well as fixed-station NO_2 data. The fixed-station NO_2 concentrations were obtained from RSQA, which manages and operated the air quality monitoring stations in the agglomeration of Montreal. The closest air quality monitoring station is Station Molson, showed in Figure 3.5, located 2.5 km away from the study corridor, and positioned at a road intersection with no other pollution sources nearby. Station Molson reports regularly on air pollutants including SO_2, NO_2, NO, O_3, $PM_{2.5}$, PM_{10} and VOCs. Note that the station is at an altitude of 15 meters above ground on the rooftop (in Figure 3.5) rather than directly at ground level, where the roadside measurements were conducted (1.2 meters).

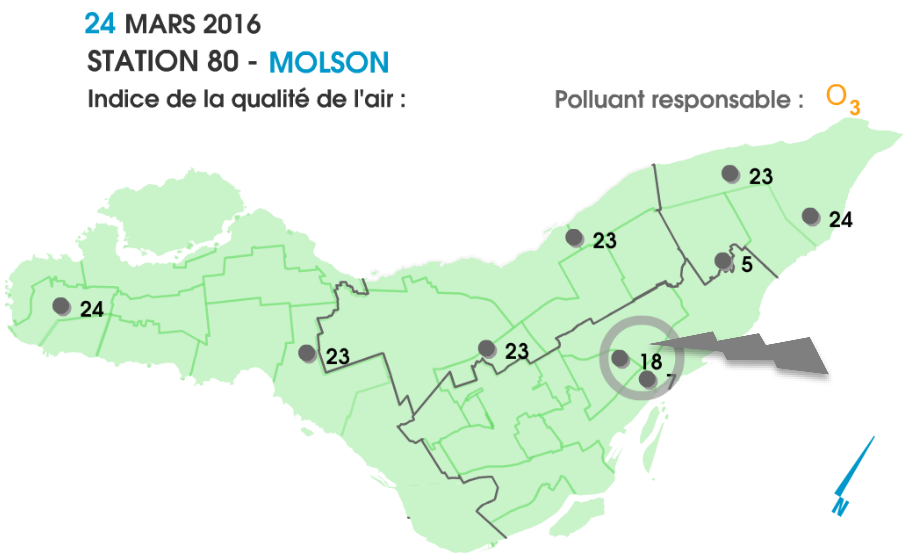

Figure 3.5: Location and Monitoring Station Molson (Source: RSQA)

3.3.3 Land Use Data Collection

To facilitate the development of dispersion models, land use data concerning each specific segment were collected and processed using a combination of ArcGIS (ArcMap 10.1, ESRI Inc.) and Google Earth (Google Inc.). All the Arc GIS shapefiles were extracted from the TRAM Archive (Transportation Research Group at McGill University) as shown in Table 3.4.

Table 3.4: GIS Data Resources Table

Name	Source	File Type
Building Footprint (municipality)	DMTI Spatial Inc.	Shapefile
General Land Use (2007)	DMTI Spatial Inc.	Shapefile
Park and Sport	DMTI Spatial Inc.	Shapefile
Street (line)	DMTI Spatial Inc.	Shapefile

Several land use and built environmental variables of interest were deducted with the aforementioned GIS shapefiles, including the building coverage, road network configuration, building heights, the presence of parks, parking lots and other open areas.

3.4 Conclusion

This chapter described the *in-situ* data collection and fixed-station data collection campaigns. *In-situ* data collection provided important meteorological parameters (temperature and relative humidity), traffic records and roadside NO_2 concentrations. The instruments used in this campaign and data collection protocols were also presented. Fixed-station data included the data of ambient NO_2 concentrations and wind profiles. Data collected in the campaigns not only provided critical inputs for the dispersion modeling chain but also was employed as a benchmark for further model validation, evaluation and inter-comparison.

CHAPTER 4 DATA PROCESSING

4.1 Introduction

Data processing was conducted following *in-situ* and fixed-station data collection campaigns. The collected data contains different formats, including texts, sheets, pictures and video recordings at various time intervals that are difficult to synchronize. Thus, the details of data processing are presented in this chapter. The processed data included traffic monitoring video recordings at intersections, meteorological data collected from the portable weather station and fixed McTavish weather station, and NO_2 concentrations detected on-site and at the fixed station Molson.

Section 4.2 provides a detailed description of how traffic video recordings were manually counted with a specific classification method. Section 4.3 introduces the spatial and temporal synchronization of data collected from fixed station and on site. Finally, Section 4.4 presents the synchronization, correction, and averaging of NO_2 concentrations measured on-site and at the fixed station. The preliminary results obtained during data processing are also presented in this chapter.

4.2 Traffic Data Processing

4.2.1 Manual Traffic Counts

With video records collected from three intersections mentioned in Section 3.2, the traffic volumes and turning routes were manually counted with great efforts. Before the manual traffic counting started, it was important to determine how to classify vehicle types to facilitate our further utility of counting results. As we were going to utilize the United States Environmental Protection Agency's Motor Vehicle Emission Simulator (MOVES 2010b to be specific, detailed introduction to the software in Chapter 5), the whole traffic counting was based on the vehicle classification mechanism embedded in MOVES 2010b (U.S. Environmental Protection Agency 2012). The vehicle classification scheme in MOVES was derived from US Department of Transportation Highway Performance. It contained 13 different categories called source type in MOVES terminology, presented in Table 4.1.

During the traffic counting procedure, we found that the definitions of passenger cars (sedans, SUVs), passenger trucks (Pickups mainly) and light-duty trucks were ambiguous. It happened that different individuals classify the same vehicles into different categories. Bias was caused during the counting procedure. However, the impact of this bias on emission estimation can be neglected. In a new version of MOVES (2014), any input for passenger cars and other light-duty trucks is now entered as light-duty vehicles, since these have evolved over time with the physical characteristics of 'cars' and 'trucks' becoming less distinct.

Table 4.1: MOVES2010b On-road Source Types (source: US EPA)

Source Type ID	Source Type Name
11	Motorcycles
21	Passenger Cars
31	Passenger Trucks (primarily personal use)
32	Light Commercial Trucks
41	Intercity Buses
42	Transit Buses
43	School Buses
51	Refuse Trucks
52	Single Unit Short-haul Trucks
53	Single Unit Long-haul Trucks
54	Motor Homes
61	Combination Short-haul Trucks
62	Combination Long-haul Trucks

According to the vehicle classification system provided by MOVES and necessary turning rules and routing decisions at each intersection, summary tables for traffic data were developed. Motorcycles, intercity buses, refuse trucks, motor homes, combination short-haul trucks and combination long-haul trucks were omitted from the counting table due to their extremely low frequency. Traffic data were conducted first in 15-min intervals due to the high capacity of the selected corridor, and then summarized into hourly traffic, thus yielded two observations per time period (each sampling round lasted 2 hours).

4.2.2 Traffic Counting Results

Traffic pattern on the selected corridor was captured by camcorders at intersections and traffic volume and vehicle types were classified and summarized into 7 categories based on their appearance. The descriptive statistics for the traffic counting results are presented in Table 4.2.

Table 4.2: Descriptive Statistics for Hourly Traffic

Variable	Mean	Min	Max
Passenger Car	773.56	272	1512
Passenger Truck	366.52	108	700
Light Commercial Truck	18.52	0	60
Transit Bus	7.88	0	28
School Bus	1.64	0	16
Single Unit Short-Haul Truck	6.24	0	28
Single Unit Long-Haul Truck	3.12	0	28
Total	1177.48	380	2372

During the analysis of traffic counting data, the morning and afternoon peak hours were noticeably observed. It was also found that afternoon peak hour on the selected corridor usually comes between 14:00-15:00, which is slightly earlier than common afternoon peak hour.

The total volume in one hour ranges from 380 (observed around noon) to 2372 (observed during morning peak), while passenger cars and passenger trucks take the major part of traffic volume (70%).

4.3 Meteorological Data Synchronization

The meteorological data used in this thesis have two sources. Temperature (in Celsius) and relative humidity were collected on-site with a portable weather station. As dispersion modeling in street canyon demands wind profiles over the roof-top, wind direction and wind speed were retrieved from McTavish Automated Reporting Station on McGill downtown campus, which is approximately 4 kilometers from the study site. Data collected on-site by a portable weather station were recorded in 15-min intervals and fixed-station data were available in 1-hour intervals. On-site data were then synchronized and averaged with fixed-station data with 1-hour intervals. It is valid to average temperature and relative humidity over a longer time period while it causes more biases to do the same with wind directions.

Among meteorological factors, it is known that the wind profile contributes more to the performance of dispersion models. The records from the McTavish Automated Reporting Station represent the wind direction of the mean wind during the specific measuring time with the resolution of one degree with respect to true north. The orientation of Papineau Avenue was measured with respect to true north using Google Earth. True north was defined as 0 degree, east as 90 degrees, south as 180 degrees and west as 270 degrees. The angle between true north and Papineau Avenue was therefore defined as 125 degrees or 305 degrees. To unify the use of street orientation, we arbitrarily deemed the angle of Papineau Avenue was 305 degrees as shown in Figure 4.1.

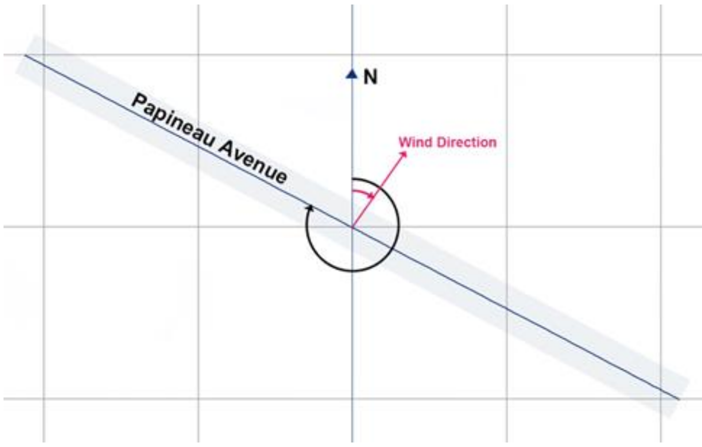

Figure 4.1: Definition of Street Orientation

With the definition of wind direction being clarified, the descriptive statistics of concerning meteorological variables were summarized in Table 4.3. The temperature and relative humidity retrieved from fixed stations were also listed to compare against our *in-situ* measurements.

Table 4.3: Descriptive Statistics for Meteorological Data

Measured items	Units	Mean	Standard deviation	Min	Max
Temperature (from portable station)	Celsius	1.63	5.67	-15.3	13.3
Relative Humidity (from portable station)	%	58.73	26.21	17.0	99.0
Temperature (from fixed station)	Celsius	-0.43	6.05	-16.0	12.0
Relative Humidity (from fixed station)	%	73.07	17.14	36.0	99.0
Wind Speed (from fixed station)	m/s	1.53	0.63	0.4	4.0
Wind Direction (from fixed station)	Degree	186.54	86.61	0.0	357.0

The records of temperature and relative humidity from the portable weather station and fixed weather station were highly correlated. Especially, measured on-site temperature ranging from -15.3 Celsius to 13.3 Celsius, with a mean value of 1.63 Celsius, while the fixed-station temperature ranging from -16.0 Celsius to 12.0 Celsius, with a mean value of -0.43 Celsius.

Wind speed from the fixed station ranges from 0.4 m/s to 4.0 m/s, with a mean value of 0.63 m/s, which demonstrates that the wind speed over the entire measurement campaign period was relatively low. The wind profile was summarized into 8 wind roses shown in Figure 4.2 for 8 measurement time slots. Also, the 8 time slots were associated with different hours of traffic simulation, which will be presented in Chapter 5. The wind speed ranges from 0.8 m/s to higher than 2.8 m/s, with speeds lower than 0.8 m/s as calm conditions.

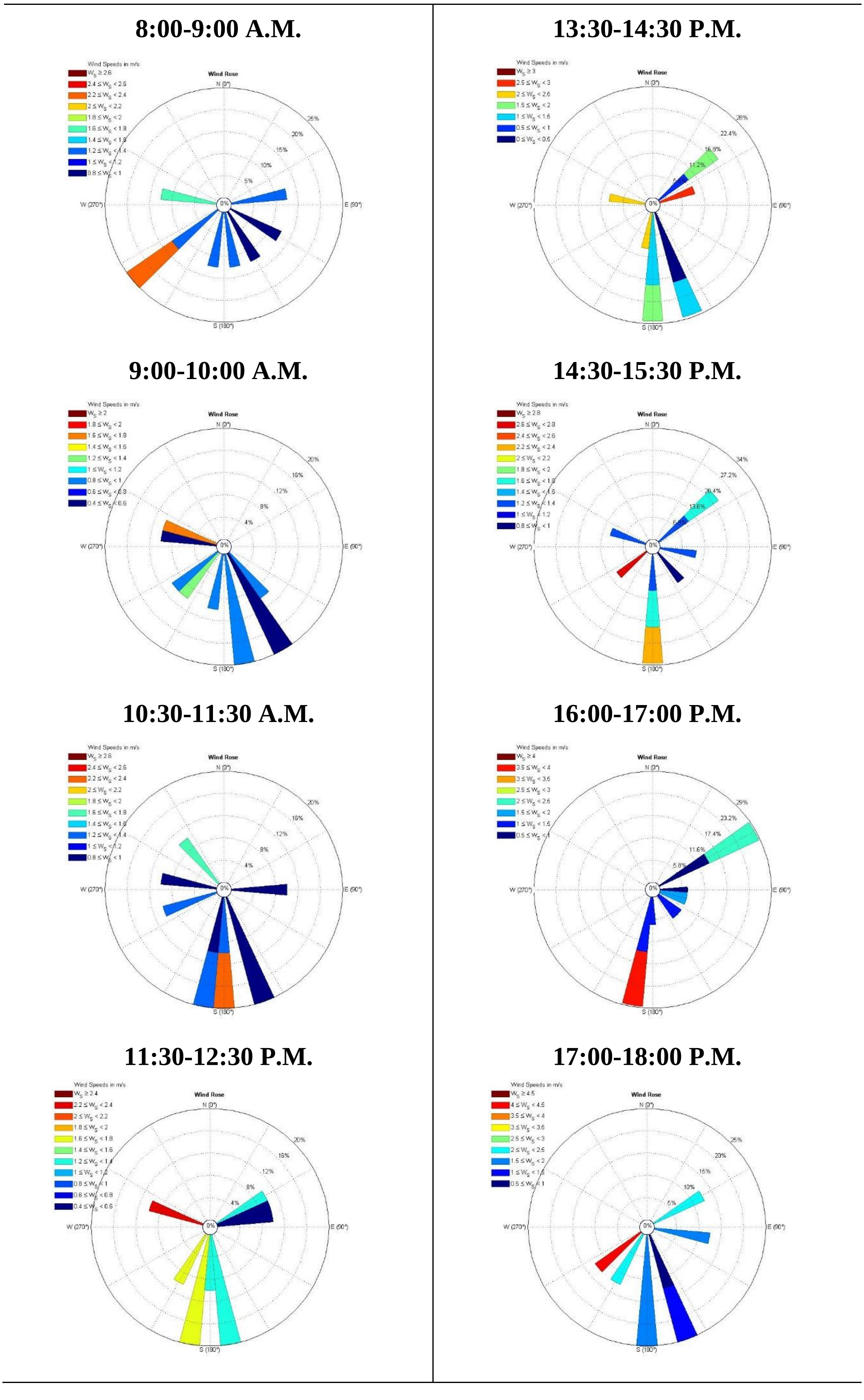

Figure 4.2: Wind Profiles during the Campaign in Each Time Period at McTavish Station

Judging from Figure 4.2, it can be concluded that during the data collection campaign, the wind blew predominantly from the south. In general, the majority of the wind speeds were less than 2.5 m/s. In order to have a better perspective of the performance of dispersion models under different meteorological conditions, we combined all wind directions (0 to 359 degrees) and wind speeds (8 observed cases) and obtained 2880 combinations of wind speed and direction designated into the abovementioned 8 time slots.

4.4 NO_2 Data Processing

4.4.1 NO_2 Data Cleaning and Synchronization

In-situ NO_2 concentrations were collected with Aeroqual Series 500 sensors. As in former studies conducted by other researchers in our group, a constant gap existed between *in-situ* measured and fixed-station retrieved NO_2 concentration data. Thus, the NO_2 sensors were adjusted and corrected to fit the concentrations measured by fixed air quality stations operated by the city of Montreal (Réseau de surveillance de la qualité de l'air, RSQA). The sensors were co-located with two different fixed stations (one located at the Pierre-Trudeau Airport and another located at the tip of the Montreal island and capturing the regional background) for two consecutive days at each station. A scatterplot was generated for NO_2 and another for O_3 illustrating the relationship between the values measured by the sensors and fixed stations. During the colocation campaign, the NO_2 sensors and fixed-station measurements were observed to be correlated. For this purpose, univariate linear regression models were developed to adjust the NO_2 and Ozone concentrations measured by Aeroqual sensors so that the sensor data could be corrected using the regression coefficients. For Ozone, the regression equation is:

$$O_{3\_real} = O_{3\_measured} \times 1.0464 - 2.2688 \tag{1}$$

As for NO_2, the equation is:

$$NO_{2\_real} = NO_{2\_measured} \times 1.0236 + 7.0297 \tag{2}$$

Processing of air quality data also involved dealing with the cross-sensitivity issue. In fact, NO_2 sensors measure at the same time, NO_2 and O_3, while O_3 sensors only measure the O_3 concentration itself. This cross-sensitivity phenomenon has been identified in previous studies concerning the use of Aeroqual Series 500 sensors (Mead et al. 2013; C. Lin et al. 2015). This is why during the measurement campaign we collocated both NO_2 and O_3 sensors so that we can subtract measured O_3 from measured NO_2 concentrations to obtain the NO_2 concentration. For this reason also, during the collocation campaign, NO_2 measured by Aeroqual sensors was compared with the sum of NO_2 and O_3 concentrations at fixed stations. The final measured NO_2 concentrations can be expressed as:

$$NO_{2_{final}} = NO_{2_{real}} - O_{3_{real}} = NO_{2_{measured}} \times 1.0236 - O_{3_{measured}} \times 1.0464 + 9.2985 \tag{3}$$

Inevitably, after subtracting, NO_2 concentrations are sometimes negative or smaller than 1ppb, which is the sensors' lower detection limit. Therefore, we set those negative NO_2 values as zero and values lower than 1ppb to 1ppb. The histogram of cleaned and corrected NO_2 concentrations is presented in Figure 4.3, featuring a lognormal distribution.

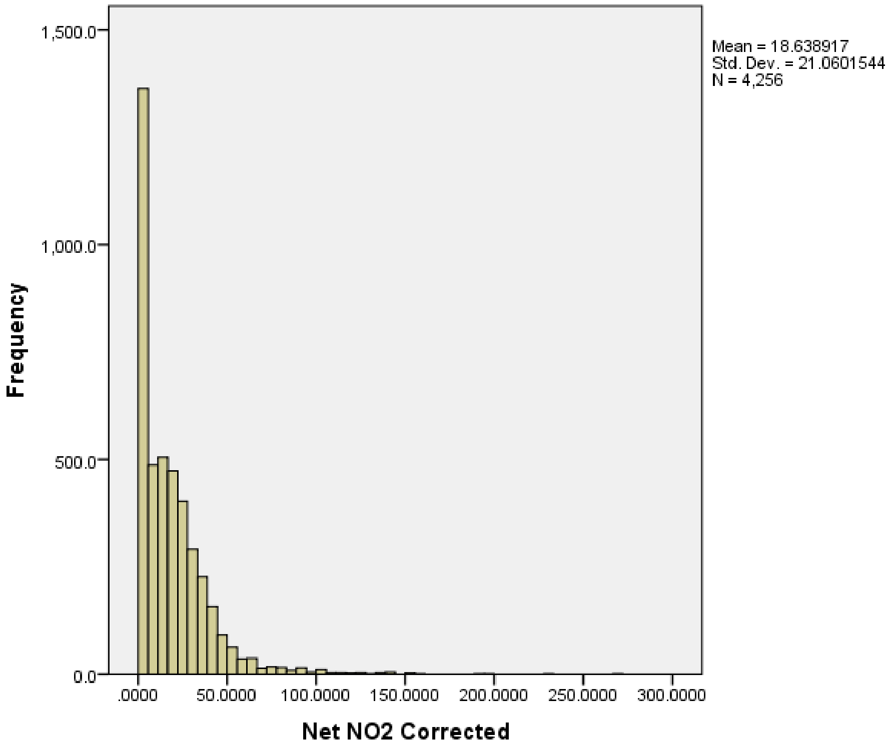

Figure 4.3: Histogram of Corrected NO_2 Concentrations

As the *in-situ* measured NO_2 concentrations were in 1-min intervals, synchronization was conducted to pair *in-situ* and fixed-station data. All *in-situ* measured and corrected NO_2 data were averaged to 1-hour intervals. Finally, we obtained 79 pairs of fixed-station and *in-situ* NO_2 values.

4.4.2 Descriptive Results for Measured NO_2 Concentrations

After data correction and synchronization, the resulting measured NO_2 concentrations were explored. Mainly, the *in-situ* measured NO_2 data were compared with fixed-station data. The hourly roadside NO_2 concentrations had a mean value of 18.64ppb and a standard deviation of 21.06ppb. Comparing with the average NO_2 concentration (9.4ppb) measured at the nearest fixed station (Station Molson) in this area during the same time period, the roadside NO_2 measured concentrations were significantly higher and exhibiting more variability and extreme values (Figure 4.4). This indicates that the fixed station cannot capture adequately the concentrations measured near-road.

Such a difference points to the importance of comparing the simulated concentrations against both roadside measurements and against the fixed-station data in order to evaluate the model performance both in the near-field and in the mid-range. Note that when we compare against the fixed-station data, the contributions of the four segments were pooled.

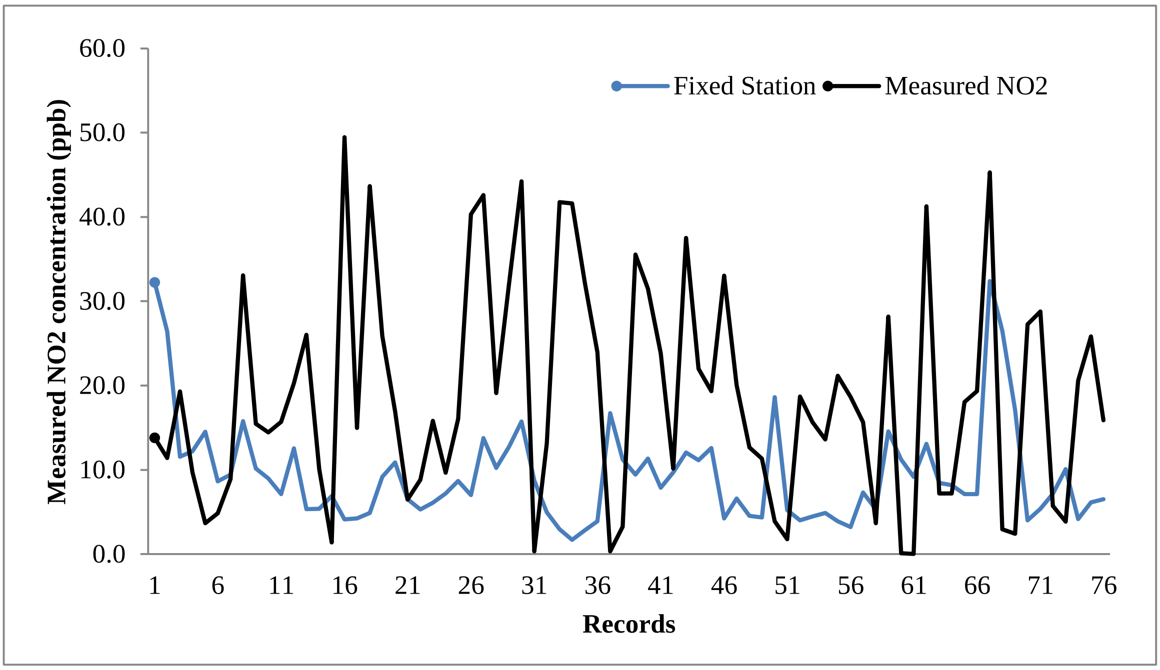

Figure 4.4: Fixed-station and Roadside Measured NO_2 Concentrations Paired in Time

The boxplot of roadside and fixed-station data was also generated (Figure 4.5). While the fixed-station data were pooled together, roadside measurements were illustrated with respect to each single segment. Therefore, the fluctuation in NO_2 concentrations caused by the different built environments at each segment was visible. Segment 3 had the highest median value. Segments 1 and 3 had the most dispersed concentration observations, while concentrations on segments 2 and 4 were less variable. Segments 1 and 4 were expected to have the highest median value as they are both lined with buildings on both sides. Segments 2 and 3 were expected to have lower NO_2 concentrations as they were one-sidedly bordered by open space. However, the on-site observations resulted in much more variability.

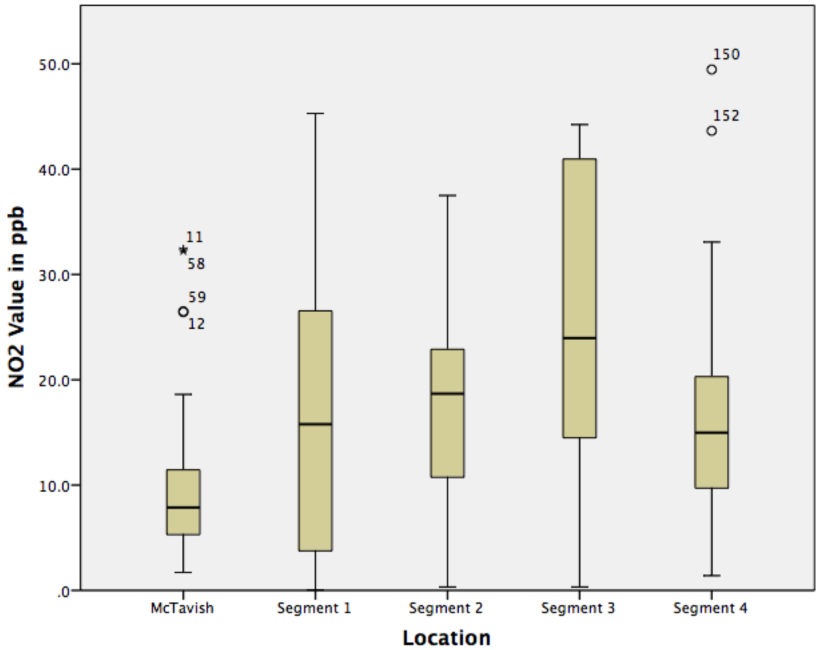

Figure 4.5: Box Plot Comparison between Fixed and In-situ Measurements

4.5 Conclusion

The data processing builds the foundation for our integrated dispersion modeling chain. The counting process of traffic recordings reproduced the traffic patterns in spreadsheets which facilitated further analysis in traffic simulation. The synchronization of meteorological data from the portable weather station and McTavish Automated Reporting Station served as a critical input for dispersion modeling. The data on NO_2 concentrations from the fixed station and *in-situ* measurements enabled the evaluation, validation and comparison of the dispersion models.

CHAPTER 5   TRAFFIC SIMULATION AND EMISSION COMPUTATION

5.1 Introduction

This chapter discusses the methodology of traffic simulation and emission computation. Traffic simulation was implemented using a micro-scopic traffic simulation software, VISSIM, to reproduce second-by-second traffic conditions along Papineau Avenue. Emission computation utilized the Motor Vehicle Emission Simulator (MOVES 2010b) developed by the US EPA, which is widely used across North America. Section 5.2 elaborates traffic simulation process by clarifying principles of traffic simulation, construction of the traffic simulation network, organization of input data. Section 5.3 introduces the emission computation procedures. This section also discusses the theory, basic settings and inputs of emission calculation.

5.2 Traffic Simulation

5.2.1 Traffic Simulation Purpose and Procedures

Microscopic traffic simulation has long been studied and evolving in numerous studies (Amirjamshidi et al. 2013; Hülsmann, Gerike, and Ketzel 2014; Clemens Mensink and Cosemans 2008; Ghafghazi 2014; Abou-Senna and Radwan 2013; Stevanovic et al. 2008; D. Lin, Yang, and Gao 2013). It spreads over the entire field of transportation research, including traffic volume estimation and prediction, driving and pedestrian behavior studies, traffic regulation planning, implementation and evaluation, traffic control, traffic safety studies and most relevant to this thesis, traffic-related air pollution studies. In this study, microscopic traffic simulation was conducted using the PTV software, VISSIM 5.40. VISSIM is a traffic simulator that can analyze transport operations under constraints such as lane configuration, vehicle composition, traffic signals, etc. It can also model pedestrian flows though not used in this study. VISSIM in this study was used to generate not only traffic volume and traffic composition of each measurement time slot but also the second-by-second traffic conditions of every single vehicle in the network. With second-by-second traffic conditions, emissions can be computed.

The implementation of VISSIM simulation started with the construction of the road network. Network orientation, segment width and length, lane configuration, traffic signals and all possible turning routes at intersections are indispensable. With a completely built road network, *in-situ* collected traffic information including traffic volume and traffic composition of each measurement time slot were inputted into the network to generate second-by-second traffic conditions and simulated traffic volume and composition as there was not much difference between traffic volumes and compositions on different weekdays at the same time slot. That is to say, we traded daily difference of traffic volumes and compositions, which can be negligible, for more precise driving patterns. Then the output of VISSIM was converted into a unified format that can be directly read by MOVES.

5.2.2 Traffic Simulation Network

As mentioned in Section 3.2.1, the overall road network included 4 streets, Rue Marie-Anne, Rue Rachel, Rue Sherbrooke, and Avenue Papineau. Rue Marie-Anne, Rue Rachel and Rue Sherbrooke divided Avenue Papineau into 3 segments. Among them, the middle segment (between Rue Sherbrooke and Rue Rachel) was actually divided into 2 smaller segments by a single-laned one-way Rue Gauthier with little traffic volume. Eventually, we divided Avenue Papineau into 4 segments of interest (Table 5.1). The streets and road segments were then further divided into 17 links. In VISSIM terminology, links are the basic units of a road network split by intersections containing several lanes running the same direction with similar characteristics and behaviors. To determine the actual orientation of the road network, a snapshot of local area from Google Earth was utilized as the background image used to draw the road network.

Table 5.1: Street Configuration Parameters (in the order from northwest to southeast)

Street Name	Segment Length (m)	Segment Width (m)	Number of Available Lanes	Direction
Rue Marie-Anne	Not applicable	14.4	4	Two-way
Papineau Segment 1	239	18	3	Two-way
Rue Rachel	Not applicable	14.4	4	Two-way
Papineau Segment 2	177	18	3	One-way
Papineau Segment 3	305	18	3	One-way
Rue Sherbrooke	Not applicable	21.6	6	Two-way
Papineau Segment 4	564	14.4	4	One-way

Turning routes were set-up based on the measurement campaign experience as well as signal controls at intersections. There are in total 17 turning routes, public transit priorities, restrictions for certain vehicle types, and traffic signals integrated in our VISSIM traffic simulation system. The final road network is presented in in Figure 5.1.

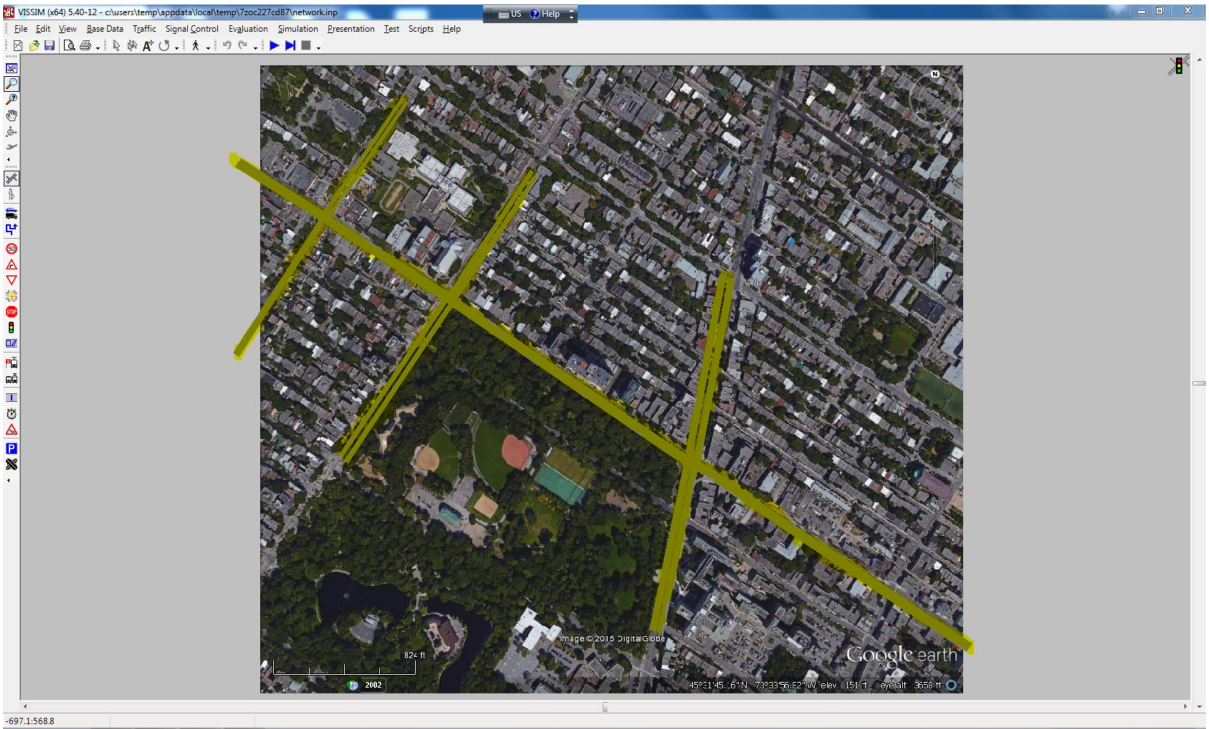

Figure 5.1: VISSIM Traffic Simulation Network

5.2.3 Organization of Traffic Simulation Inputs

In order to run traffic simulation hour by hour for each measurement time slot, traffic volume and composition were averaged over the entire data collection campaign into 8 time slots, namely 8 a.m. to 9 a.m., 9 a.m. to 10 a.m., 10 a.m. to 11 a.m., 11 a.m. to 12 p.m., 13 p.m. to 14 p.m., 14 p.m. to 15 p.m., 16 p.m. to 17 p.m. and 17 p.m. to 18 p.m. It is worth noting that, in VISSIM, the vehicle classification system is not as detailed as our manual counts. Only 3 categories are included in VISSIM, cars, heavy goods trucks and buses. We then merged the categories from our manual counts as such: passenger cars, passenger trucks and light commercial trucks as cars; transit buses and school buses as buses; and short-haul and long-haul trucks as heavy good trucks. All the results were summarized in 8 spreadsheets. Each spreadsheet contained two parts, one with the traffic composition and volume on each link to determine the in-flow and out-flow traffic of the entire network, and another with traffic at each intersection to decide the routing decision of the traffic flow.

Traffic simulation was then run hour by hour for 8 time slots corresponding to our *in-situ* data collection time slots. Each run contained 4600 seconds. At the beginning of each run, there was no vehicle in the road network and the vehicle generator at each road end started to send vehicles to the network, so that the first 1000 seconds allowed the traffic volume in the network to reach equilibrium. Simulated data were recorded from the 1001st second to 4600th second, which represented the traffic condition in a certain simulation time slot. Traffic condition was recorded on a second by second basis.

5.3 Emission Calculation

5.3.1 Total Emissions

Emissions of NO_x were modeled using the Motor Vehicle Emission Simulator (MOVES 2010b) developed by the US EPA, which is widely used across North America to estimate on-road and non-road emissions of greenhouse gases, criteria pollutants and selected air toxics (U.S. Environmental Protection Agency 2012). The MOVES model is currently the official model for use for state implementation plan (SIP) submission to EPA and for transportation conformity analyses outside of California. The model is also the primary modeling tool to estimate the impact of mobile source regulations on emission inventories. Other than regulatory uses, MOVES was also presented in numerous previous air quality studies that integrated microscopic traffic simulation and emission estimation(Zhao and Sadeka 2013; Abou-Senna et al. 2013; Xie et al. 2012; Alam and Hatzopoulou 2014).

In our case, MOVES was integrated with VISSIM to simulate second-by-second NOx emissions. MOVES requires information on link activity, link source, link information, fuel, vehicle age distribution, and averaged meteorological data. The identification of 'links' in MOVES follows that of VISSIM as well. It is also worth mentioning that no changes were made to the MOVES database of base emission rates since we can reasonably assume that the Canadian and US vehicle fleets are similar.

Link activity refers to the traffic activity occurring on the links, namely, driving cycle, traffic volume and traffic speed on a second-by-second basis. Link source refers to traffic composition on each link.

Link source refers to traffic composition and the fraction of each vehicle category. As traffic composition tends to be stable in each of our 8 time slots, link source has an interval of one hour. As mentioned in Section 5.2, VISSIM has less vehicle categories and we merged our vehicle types when running VISSIM. Before running MOVES, we collapsed the traffic again into the MOVES vehicle classification based on the VISSIM simulated traffic.

Link information refers to the length and road grades of links. Link information was input for Montreal to reflect local conditions. Link length and road grades were derived from various shapefiles using ArcGIS.

Information on fuel was obtained from the Province of Quebec. Vehicle age distribution was obtained from the Société de L'assurance Automobile du Québec (SAAQ) based on vehicle ownership records.

As such, for each link, 8 different emission cases (for our 8 time slots) were estimated, reflecting the variation of mean hourly emissions across the 8 hours. .

5.3.2 Emission Factor Calculation

The total emissions of NO_x for each specific time slot were estimated by MOVES in the unit of grams. As the length of each road link was already known, emission factors (EF) were calculated as NO_x emissions (in gram) divided by vehicle kilometers travelled (VKT) or vehicle miles travelled (VMT). The emission factors in g/VKT were later used in OSPM and g/VMT in CALINE4 to estimate NO_2 concentrations with the NO_x/NO_2 mix ratio (detailed emission factors showed in Section 8.2). The emission factors were only classified into 2 categories, one for light vehicles and another for heavy vehicles. It is worth noting that the SIRANE model requires only total emissions of each link. Thus the traffic simulation-emission computation- dispersion modeling integration has been established.

5.4 Conclusion

The methodology discussed in this chapter translates the data collected from the real world to applicable inputs for our dispersion models. Traffic simulation not only provided second-by-second traffic conditions for emission computation but also traffic information such as volume and vehicle type for dispersion models. Emission computation reproduced the total emission on each road link. Furthermore, emission factors were calculated for dispersion modeling. These methods have paved the way for the last step of our modeling chain—dispersion modeling.

CHAPTER 6 DISPERSION MODELING USING OSPM, CALINE4 AND SIRANE AND MODEL PERFORMANCE VALIDATION AND COMPARISON

6.1 Introduction

The core element of this research involves dispersion modeling using 3 different dispersion models, OSPM, CALINE4 and SIRANE. OSPM and CALINE4 are both commonly used dispersion models in Europe and North America respectively, which were validated and evaluated by numerous studies. SIRANE is a newly developed model developed by Ecole Centrale de Lyon, which has not been widely employed. This chapter focuses on the construction and running of the three dispersion models, as well as their validation and inter-comparison. Section 6.2 focuses on the OSPM dispersion modeling inputs and procedures. Sections 6.3 and 6.4 discuss CALINE4 and SIRANE. Section 6.5 elaborates the performance criteria and the derivation of a two-tier evaluation system and the inter-comparison methodology between the three models.

6.2 OSPM Dispersion Modeling

6.2.1 Introduction to OSPM

The Operational Street Pollution Model, more commonly known as OSPM model, is a widely used air pollution dispersion model specializing in modeling dispersion in urban built environments. It has been considered as state-of-the-art in applied street level pollution modeling (Kakosimos et al. 2010). It is physically built on the theory of ‘street canyon’ effect, which indicates a recirculation within a typical urban built environment as shown in Figure 6.1.

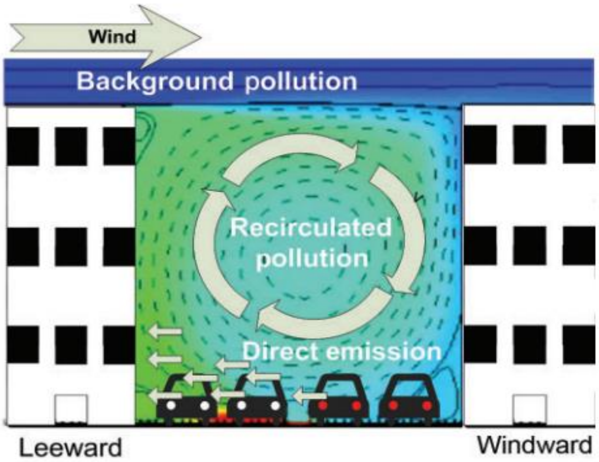

Figure 6.1: Sketch of a Typical Street Canyon

It also contains simple chemical reactions concerning the NO_2 photolysis process:

$$NO + O_3 \rightarrow NO_2 + O_2$$

$$NO_2 + hv \rightarrow NO + O$$

$$O + O_2 \rightarrow O_3$$

The OSPM model has been used in Europe for almost 20 years. Numerous modeling and validation experiments have been conducted to evaluate its performance in either long-term or short-term prediction under various local land-use and meteorological conditions (Raducan 2008; Murena et al. 2009; Jensen et al. 2013; Aquilina and Micallef 2004; Kukkonen et al. 2001). A recent application of OSPM in the city of Montreal indicated that the simulated NO_2 concentrations have a reasonable agreement with data collected at fixed stations (Ghafghazi 2014).

6.2.2 Universal Inputs

Universal inputs shared by the three models mainly contain wind profile, temperature, traffic volumes and background concentrations.

Among all universal or featured inputs, wind profile has the most significant impact on the performance of dispersion models. As described in Section 4.3, in order to have a better perspective on the performance of dispersion models under different meteorological conditions, we combined all wind directions (0 to 359 degrees) and wind speeds (8 observed cases) and obtained 2880 combinations of wind speed and direction designated into 8 simulation time slots. All the wind profile combinations were simulated in OSPM, CALINE and SIRANE.

Temperature was obtained from our portable weather station co-located with our NO_2 monitors. Daily variation in temperature was eliminated by averaging temperature over the data collection campaign for each time slot.

Traffic volume was a vital input in all the dispersion models. It was derived from hourly VISSIM traffic simulation results.

Background concentrations of NO_2, NO_x (NO_2 and NO) and O_3 in ppb were obtained from RSQA on an hourly basis.

6.2.3 OSPM Featured Inputs

OSPM also requires specific inputs that other models don't. First of all, OSPM demands description of buildings bordering the street. The description is based on a polar coordinate system with the midpoint of the road segment being the pole. That is to say, the length of buildings was expressed using angles. The length and height data of bordering buildings were obtained from shapefiles using ArcGIS.

Solar radiation was also required in OSPM to calculate the NO_2 photolysis reaction rate. In our case, solar radiation was set to a fixed number of 300 W/m^2 judging from cloud cover conditions and the season in which data collection took place.

In OSPM, traffic composition was simply classified as light vehicles and heavy vehicles. Emission factors were also processed in this manner as discussed in Section 5.3. Traffic speed was also a featured input in OSPM to introduce traffic-induced turbulence into the model.

6.3 CALINE4 Dispersion Modeling

First developed decades ago, CALINE4 has been popularized in North America as both a regulatory and research tool to study air pollutant dispersion especially on highways (Benson 1992). CALINE4 can handle several different air pollutants including CO, NO_2 and other inert gases and particles. As CALINE4 is a line source Gaussian model, it has several inherited shortcomings especially the limitation under low wind speed and almost parallel winds (Benson 1992; Levitin et al. 2005; Wallace and Kanaroglou 2008), and when receptors are placed close to the line source (Wallace and Kanaroglou 2008).

Different from OSPM and SIRANE, CALINE4 is the only model out of the three that was not specifically developed for urban canyons. Therefore, it neglects the effects of buildings along the road. However, as we selected two road links with open area on one side, CALINE4 has the possibility of performing reasonably well for these two segments. CALINE4 also employs the same simplified NO_x chemistry as OSPM and SIRANE (Benson 1992).

Other than the aforementioned universal inputs, CALINE4 requires specific inputs. Firstly, CALINE4 as well as SIRANE require atmospheric stability class (in our case, Pasquill Stability Class). The Pasquill Stability Classes are shown in Table 6.1. We arbitrarily picked neutral conditions with wind direction standard deviation being 10 degrees to represent the atmospheric conditions over the period of our data collection campaign.

Table 6.1: Pasquill Stability Class Paired with Wind Direction Standard Deviation

Pasquill Stability Class	Conditions	Wind Direction St. D (Degree)
A	Extremely unstable	25
B	Moderately unstable	20
C	Slightly unstable	15
D	Neutral	10
E	Slightly stable	5
F	Moderately stable	2.5
G	Extremely stable	1.7

CALINE4 also embeds the NO_2 photolysis reactions as in OSPM. The NO_2 photolysis reaction rate was a required input in CALINE4. With NO_2 photolysis rate being set to 0, our CALINE4 model simulated the most conservative situation with the highest possible NO_2 concentration.

As mentioned Section 5.3, CALINE4 pooled all the traffic composition together. Thus, only a total traffic volume and an averaged emission factor were required for each road segment.

CALINE4 doesn't contain any information on built environment. The road geometry in CALINE4 was expressed with Cartesian coordinate system. According to the length and orientation of Papineau Avenue, it was simple to build the simulation network.

6.4 SIRANE Dispersion Modeling

SIRANE made use of the link total emissions generated from MOVES without calculating emission factors. As a recently developed dispersion model, SIRANE has several new characteristics that distinguish it from others. SIRANE simulates each street with a box model and calculates the corresponding advective fluxes balance at intersections (Soulhac et al.). This model accounts for three important transport mechanisms within the urban canopy to better estimate the effect of the complex street configuration in an urban area: 1) advective mass transfer along the street due to the mean wind along the axis, 2) turbulence mass transfer across the interface between the street and the overlying atmospheric boundary layer, and 3) advective transport at street intersections (this last term is not treated by OSPM or CALINE4). Also SIRANE adopts the classic NO_x photochemical process as the former two models. SIRANE has different treatment of links with or without buildings on both sides which makes it ideal for our case (Soulhac et al.).

The inputs of SIRANE model were generally the same as OSPM and CALINE4, including pollutant emissions, background concentrations, meteorological data and building configuration data from GIS as well as a list of other parameters such as latitude, district aerodynamic roughness, albedo, Priestley-Taylor coefficient, washout rate, etc.

6.5 Validation and Inter-Comparison of Dispersion Models

OSPM, CALINE and SIRANE were run under the same emission and meteorological conditions to simulate NO_2 concentrations at four different receptors; each receptor located midblock on the side of each road segment. Since unified evaluation system was used in this thesis, it enabled the inter-comparison between the three dispersion models.

The simulated NO_2 concentrations at each of the four receptors were paired with measured NO_2 concentrations at the same receptor location and under the same traffic and meteorological conditions. This leads to about 20 pairs of observed-simulated data for each segment and for each dispersion model. In total 240 pairs (3 models' results * 4 segments * 20 paired data each segment) of observed-simulated data were analyzed.

The simulated results were also matched with measurements conducted at a fixed monitoring station managed and operated by the City of Montreal through the air quality surveillance network (RSQA). Station 80, located 2.5 km away from study corridor was used for this comparative exercise. Note that the station is at an altitude of 15 meters above ground rather than directly at ground level, where the roadside measurements were conducted (1.2 meters). To conduct this comparison, NO_2 concentrations were simulated after accounting for the emissions from the four road segments simultaneously.

Validation of simulated concentrations was performed using a set of acceptance criteria initially proposed by Chang and Hanna(Chang and Hanna 2004) for the evaluation of dispersion models against *in-situ* observations (Table 6.2). These model performance measures and criteria were later evaluated and validated in the literature (Kenty et al. 2007;

Hanna and Chang 2012) . In Table 6.2, C represents the concentration; the subscripts s and o refer to simulated and observed concentrations and the over bar represents an average.

Table 6.2: Summary of Performance Measures for Dispersion Model Validation

Performance Measures	Definition	Ideal Value	Rural Criterion	Urban Criterion
Absolute Fractional mean Bias (FB)	FB= $\boldsymbol{2(\overline{C_o}-\overline{C_s})/(\overline{C_o}+\overline{C_s})}$	0	<0.3	<0.67
Normalized Mean-Square Error (NMSE)	NMSE= $\boldsymbol{\overline{((C_o-C_s)^2)}/(\overline{C_o}\cdot\overline{C_s})}$	0	<3	<6
Normalized Absolute Difference (NAD)	NAD= $\boldsymbol{\overline{\lvert C_o-C_s\rvert}/(\overline{C_o}+\overline{C_s})}$	0	<0.3	<0.6
Fraction of C_s within a factor of two of C_o (FAC2)	Fraction where $\boldsymbol{0.5<\frac{C_s}{C_o}<2}$	1	>0.5	>0.3
Geometric Mean Bias (MG)	MG=$\boldsymbol{exp(\overline{lnC_o}-\overline{lnC_s})}$	1	0.7<MG<1.3	
Geometric Mean Variance (VG)	VG=$\boldsymbol{exp\overline{(lnC_o-lnC_s)^2}}$	1	0.4<VG<1.6	
Correlation Coefficient	Pearson Correlation Coefficient	1	-	-

According to the definitions, FB, NMSE and NAD would ideally equal 0 while FAC2, MG, VG and the correlation coefficient would ideally equal 1 for a perfect model. In the study presented by Hanna and Chang (Hanna and Chang 2012), two sets of acceptance criteria (one for rural areas and the other for urban areas) were documented. As shown in Table 6.2, the rural criteria are more stringent than urban ones. By setting the urban criteria as lower level performance standards and the rural criteria as higher-level standards, we use both sets of acceptance criteria to evaluate our models.

6.6 Conclusion

This chapter discusses the construction of three dispersion models VISSIM, CALINE4 and SIRANE with well-formatted inputs from previous data processing, traffic simulation and emission computation, which is the core component of this thesis. It also presents the evaluation, validation, and comparison of the three dispersion models' performance using the unified evaluation acceptance measures proposed by Hanna and Chang (2004). Lower and higher-level criteria were set using urban and rural standards for dispersion models mentioned in their study (2012). The construction of dispersion models primarily depends on the universal inputs, including land use data, meteorological data, traffic data and emission data (emission factors or total emission), despite their slight differences in formatting. These models also require unique inputs such as relative humidity, solar radiation, NO_2 photolysis rate, etc. Once the simulation was done, the results were collapsed and paired with *in-situ* measured and fixed-station NO_2 concentrations for model validation and inter-comparison.

CHAPTER 7 RESULTS AND DISCUSSIONS

7.1 Introduction

This chapter analyzes the results of the integrated traffic-emissions-dispersion models. Section 7.2 discusses the traffic simulation and emission calculation results. Traffic simulation was summarized as hourly traffic volume and composition. Section 7.3 elaborates the dispersion modeling results and finally, Section 7.4 explores and presents the validation and inter-comparison between dispersion models' performance.

7.2 Traffic Simulation and Emission Calculation

7.2.1 Traffic Simulation Results

Traffic conditions were simulated and recorded for 8 time slots corresponding to our field measurements. Note that the aim of our traffic simulation is to serve the demands of emission computation and dispersion modeling. The hour-by-hour output of traffic simulation results from VISSIM was summarized into 8 spreadsheets that can be read by MOVES. The spreadsheets mainly contained three parts. The first part encompassed the information of second-by-second traffic volume, traffic composition and traffic speed on the 17 links in the simulated time slot. The second part contained the aggregated traffic volume and averaged traffic speed on the 17 links over the simulated hour. The third part was explanatory and complementary information for the spreadsheet, e.g. abbreviations and units.

To validate the effectiveness of our traffic simulation system, a comparison was made between simulated and observed traffic volumes. Note that, as simulated traffic volumes represented an average volume in each time slot over the data collection campaign, the observed data were also averaged over the same time period. Traffic volume comparison results can be found in Figure 7.1 for the four segments (segment 2 and segment 3 shared the same traffic volume in Figure 7.1(b)) and 8 time slots. These two sets of data showed strong correlation and also reflected urban traffic characteristics with morning and afternoon peaks at 8:00-9:00am and 14:00-15:00pm and lower volumes in the midday. This also justified our use of simulated traffic information to represent average traffic conditions on an average weekday.

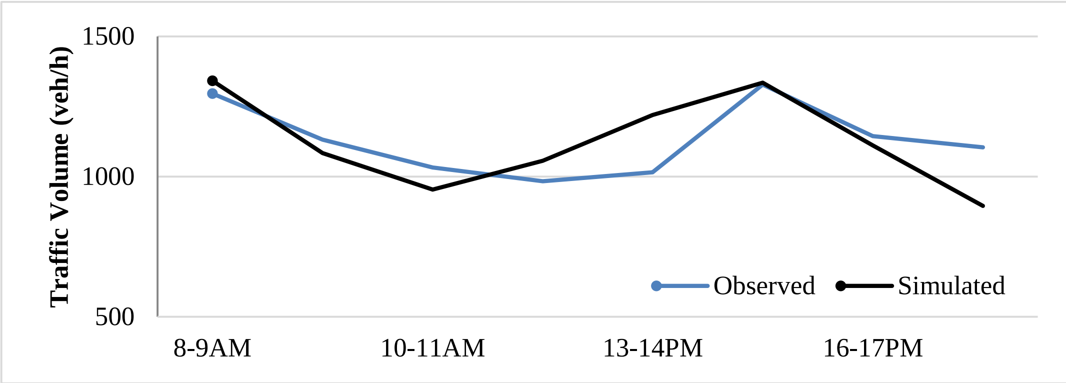

(a)

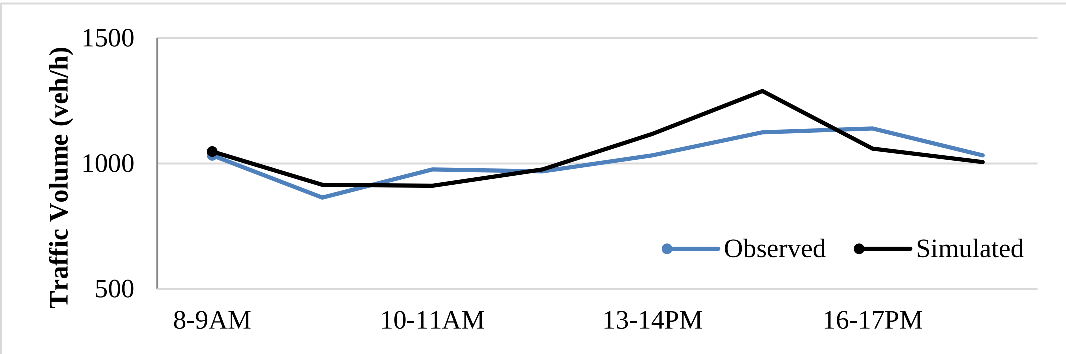

(b)

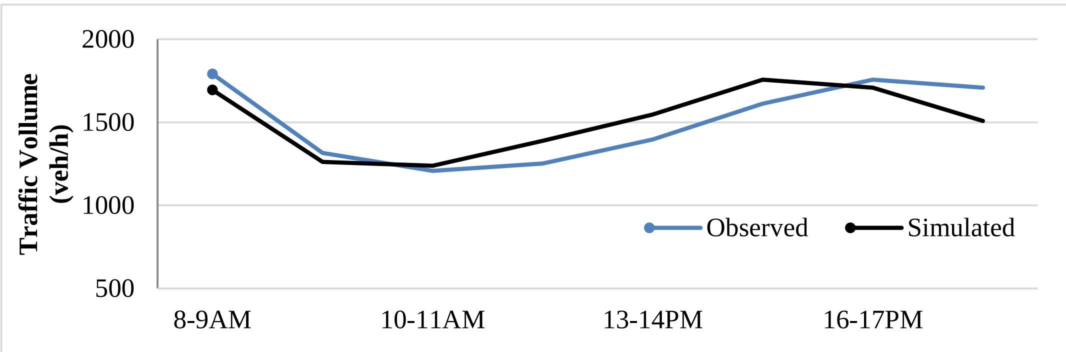

(c)

Figure 7.1: Comparison between Simulated and Observed Traffic Volumes at Segment 1 (a), Segment 2 and 3 (b), and Segment 4 (c)

7.2.2 Emission Calculation Results

As total emissions of NOx on each link calculated by MOVES can only directly serve as an input for SIRANE model. They were later translated into emission factors for each specific time slot. As the length of each road link was already known, emission factors (EF) were calculated as NO_x emissions (in gram) divided by vehicle kilometers travelled (VKT) or vehicle miles travelled (VMT). The emission factors were only classified into 2 categories, one for light vehicles and another for heavy vehicles. The detailed emission factors are shown in Table 7.1.

Table 7.1: Emission Factors with Respect to 8 Time Slots and 4 Road Segments

	Location 1 EF (g/VKT)		Location 2, 3 EF (g/VKT)		Location 4 EF (g/VKT)	
Time Slot	Light Vehicle	Heavy Vehicle	Light Vehicle	Heavy Vehicle	Light Vehicle	Heavy Vehicle
8-9AM	0.458	10.342	0.41	8.181	0.119	1.017
9-10AM	0.391	9.667	0.331	6.888	0.125	0.973
10-11AM	0.47	10.229	0.337	6.434	0.129	1.045
11-12PM	0.455	9.94	0.342	6.331	0.123	1.011
13-14PM	0.467	11.564	0.359	7.506	0.129	1.093
14-15PM	0.477	13.672	0.353	7.643	0.129	1.229
16-17PM	0.454	14.678	0.322	8.133	0.108	1.34
17-18PM	0.485	14.416	0.278	5.619	0.093	1.107

7.3 Dispersion Modeling Results

NO_2 concentrations on each link were simulated for each of the four segments, under different time periods and various wind speeds and direction combinations as presented in Section 4.3, leading to a total of 2880 runs completed by each of the three models. Simulated

NO_2 concentration reflected an hourly average concentration for each segment in a specific time slot under all possible meteorological cases. Only when the simulated and observed data had the same wind profile and other meteorological conditions, we paired them together. We finally ended up with a total of 79 paired dispersion simulations and measurement data.

Figure 7.2 illustrates the variation between measured and simulated results. Roadside measurements have more variability than simulated values (and more variability that fixed-station measurement as pointed out earlier). This indicates that the dispersion models are unable to capture the entire variability in measured concentrations (due to short-term peaks caused by long queues or a large amount of heavy vehicles passing, etc).

While OSPM and CALINE4 simulate almost the same concentrations along each of the four segments, the behavior of SIRANE is different. We observe that concentrations simulated by SIRANE at segments 1 and 4 are very different from the concentrations simulated at segments 2 and 3. SIRANE, simulated concentrations at segments 1 and 4 that are higher than the concentrations that it simulated at segments 2 and 3. Indeed, this is expected as these two links (1 and 4) have buildings on both sides with an aspect ratio of 0.6. Overall, the three models failed to capture the extreme values that were captured by roadside measurements and generally underestimated the concentrations measured near the road. The mean values simulated by each of the three models were closer to the fixed-station data (9.4ppb compared to 11.7, 13.9 and 16ppb for OSPM, CALINE and SIRANE respectively). This indicates that simulated concentrations seem to better represent “average” conditions rather than extreme events affecting near-road concentrations.

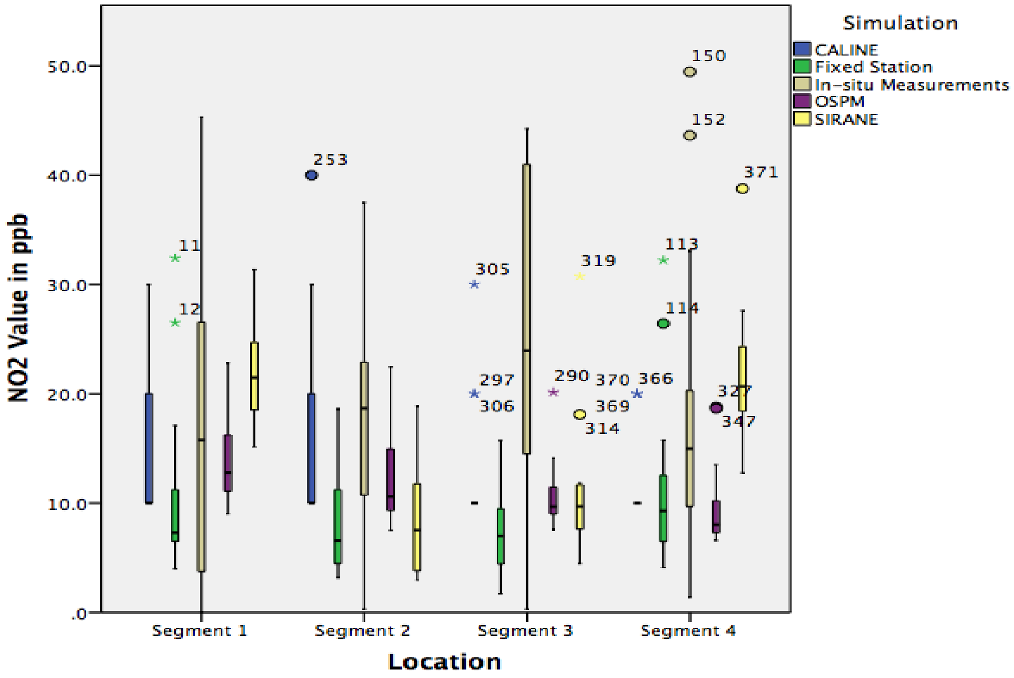

Figure 7.2: Box Plot of Simulated Results

7.4 Dispersion Modeling Validation and Inter-Comparison Results

To validate the results of dispersion, a set of performance measures and acceptance criteria were adopted. The rural and urban acceptance criteria proposed by Hanna and Chang (Hanna and Chang 2012; Chang and Hanna 2004) were set as higher and lower level criteria respectively, with the rural criterion being more stringent. Both roadside measurements and fixed-station data were used to conduct the validation. Table 7.2 and 7.3 summarize the results of our validation exercise.

When validating against roadside measurements, all the three models seemed to exhibit the best performance at segment 1 which is lined by buildings on both sides with an aspect ratio of 0.6. OSPM performed better than the other two at segment 1 (a street canyon) and much worse at segments 2, 3 and 4. SIRANE had the best overall performance among the three and especially along segments 1 and 4; its fractional bias values were smaller than 0.1 (0.08 and

0.06 respectively). CALINE performed better than the other two models at segments 2 and 3. Not surprisingly, both segments have the lowest building density with open area on one side and buildings on the other side.

Comparing to fixed-station data, the SIRANE model still demonstrated the best overall performance. Judging from the FAC2 values, shown in Figure 7.3, all three models had better agreement with fixed-station data rather than roadside measurements. The green lines indicated FAC2 values equal to 0.5(lower) or 2 (upper). And the red line indicated the FAC2 value equal to 1. Also the three models showed better correlation with fixed-station data.

It is worth noticing that though the most MG and VG values didn't comply with the acceptance criteria, MG and VG were not used in the study that presented them as performance measures. In Hanna and Chang's study, only FB, NMSE, FAC2 and NAD were used to evaluate the overall performance of air dispersion models. A good dispersion model should satisfy more than half of the time the four acceptance criteria proposed above in independent runs, in our case, simulation for each segment. As a result, the comprehensive acceptance measure of OSPM, CALINE4 and SIRANE all exceeds 0.875 (0.875, 0.938, 0.875 respectively) under urban criteria (lower-level criteria), and 0.375 (0.375, 0.5, 0.5) under rural criteria (higher-level criteria). It indicates that the application of OSPM, CALINE4 and SIRANE is acceptable for our case in an urban area, while CALINE4 and SIRANE showed better performance.

Table 7.2: Validation against Roadside Measurements

Segment	Simulation	|FB|[a]	NMSE[a]	FAC2[b]	NAD[a]	MG[b]	VG[b]	Pearson[b]
1	**OSPM**	0.37*	1.87**	0.48*	0.43*	0.61	34.48	0.463
	CALINE	0.26**	1.50**	0.33*	0.43*	0.58	33.6	0.49
	SIRANE	0.08**	1.34**	0.52**	0.38*	0.38	72.05	-0.05
2	**OSPM**	0.46*	1.27**	0.52**	0.42*	1.12[c]	6.36	-0.296
	CALINE	0.26**	1.29**	0.52**	0.43*	0.97[c]	8.22	-0.387
	SIRANE	0.83	2.14**	0.33*	0.50*	1.92	8.8	0.11
3	**OSPM**	0.82	1.54**	0.33*	0.46*	1.72	6.75	0.106
	CALINE	0.67	1.25**	0.4*	0.44*	1.51	7.49	-0.034
	SIRANE	0.79	1.54**	0.40*	0.45*	1.83	5.52	0.11
4	**OSPM**	0.69	2.02**	0.52**	0.45*	1.56	2.88	-0.098
	CALINE	0.50*	1.54**	0.5**	0.39*	1.26	2.5	-0.197
	SIRANE	0.06**	0.80**	0.54**	0.34*	0.7[c]	2.9	-0.23
Pooled	**OSPM**	0.57*	1.69**	0.48*	0.44*	1.13[c]	8.08	0.08
	CALINE	0.41*	1.39**	0.44*	0.42*	0.99[c]	8.42	0.026
	SIRANE	0.27**	1.27**	0.46*	0.40*	0.94[c]	10.34	-0.06

a: The ideal value for this criterion is 0; b: The ideal value for this criterion is 1;

c: recommended value between [0.7, 1.3]

*: Complying with lower level acceptance criterion

**: Complying with higher level acceptance criterion

Table 7.3: Validation against Fixed-station Data

Simulation	|FB|[a]	NMSE[a]	FAC2[b]	NAD[a]	MG[b]	VG[b]	Pearson[b]
OSPM	0.22**	1.06**	0.47*	0.37*	1.55	2.35	-0.25
CALINE	0.39*	0.83**	0.56**	0.40*	1.28	2.04	-0.37
SIRANE	0.20**	0.84**	0.59**	0.37*	1.23[c]	3	-0.19

a: The ideal value for this criterion is 0; b: The ideal value for this criterion is 1;

c: recommended value between [0.7, 1.3]

*: Complying with lower level acceptance criterion

**: Complying with higher level acceptance criterion

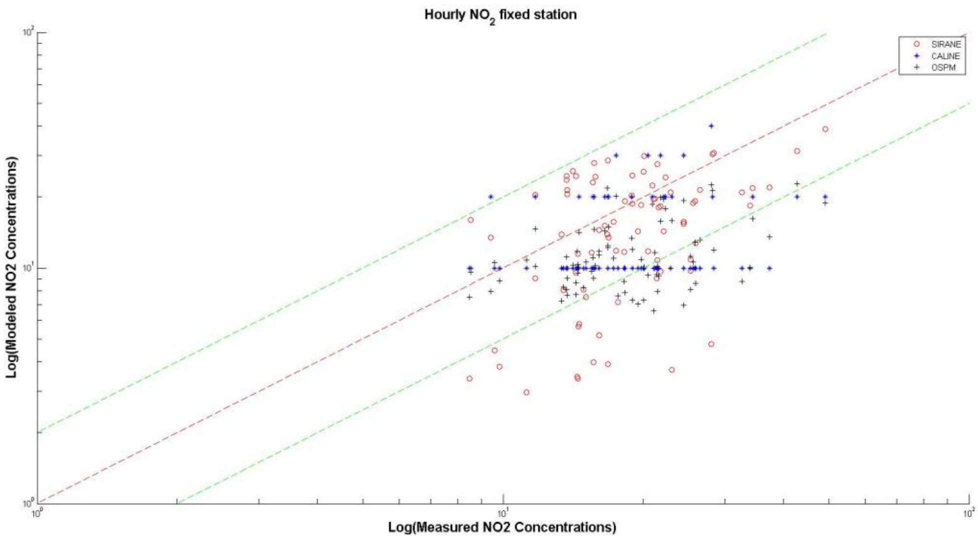

Figure 7.3: Scatter Plot of Simulated vs. Measured Concentrations

7.5 Discussion

7.5.1 Fixed-station and Roadside Measurements

As demonstrated in 3.1, roadside measurements and fixed-station data showed notable differences, which encouraged us to employ both data sets to validate our simulation results. The reasons leading to this phenomenon include: 1) Fixed-station monitor is placed on a rooftop over 15 meters above street level while our portable monitors were positioned 1.2 meters above ground and close to the curb thus capturing the effects of prompt traffic changes. 2) The measurement campaign took place in late March and early April. The local temperature during this period stayed below zero Celsius. The influence of domestic heating must be considered. Emissions from both traffic and domestic heating may be more easily trapped in a street canyon due low wind speed conditions, which led to higher roadside concentrations. 3) Aeroqual monitors are also prone to error.

7.5.2 Dispersion Model Performance at Different Locations

We selected 4 segments that have different built environments to examine the performances of these three dispersion models. Though all three dispersion models have satisfying performance comparing with roadside and fixed-station data, it can be noticed that between these road segments, all the three models showed good agreement with roadside data at segment 1 that has buildings on both sides with an aspect ratio bigger than 0.5 and poor agreement at segment 3 that has tall buildings on one side and open area on the other side. The reason lies in that OSPM and SIRANE were originally designed to simulate dispersion in street canyons with aspect ratio larger than 0.5 and 0.33 respectively (Benson; Soulhac et al.). The SIRANE model had the best performance at segments 1 and 4 (with buildings on both sides) compared with roadside data and moderate performance at segments 2 and 3 (with park on one side). We observe that as SIRANE treats one-side-building segments and street canyon segments in different manners, there is an apparent concentration variance between segments 1,4 and segments 2,3, which was hardly detected in OSPM and CALINE. Validating again fixed-station data, we also observe the same trend that SIRANE has a better performance. Among these three models, CALINE is the only one not specifically designed for street canyon simulation. However, what is noticeable is that CALINE had the best performance among the three at segments 2 and 3, which had the lowest building density and bordered one-sidedly by open space. This built environment is very similar to open terrain, in which CALINE was designed to work and has the best performance.

7.5.3 Dispersion Model Performance under Different Meteorological Conditions

It has been found in previous literature (Kakosimos et al. 2010; Benson 1992; Wallace and Kanaroglou 2008; Levitin et al. 2005) that for OSPM and CALINE models, they have better performance with high wind velocity. Mostly the wind speed should be higher than 1.5 meter per second. Some studies regarding the evaluation of CALINE model even excluded the conditions with wind speeds smaller than 0.5 m/s (Levitin et al. 2005). SIRANE is also limited in terms of its performance to simulate dispersion under calm winds (Soulhac et al.). In Table 7.4, we can conclude that for most situations, these three models, especially OSPM and CALINE models, perform better when the wind speed is higher than 1.5 m/s.

Table 7.4: Comparison between Different Wind Speeds

Wind speed			FB	FAC2
Fixed-station	>1.5 m/s	OSPM	-0.25	0.9
		CALINE	-0.31	0.8
		SIRANE	-0.7	0.5
	<1 m/s	OSPM	-0.37	0.625
		CALINE	-0.65	0.33
		SIRANE	-0.39	0.625
Roadside measurements	>1.5 m/s	OSPM	0.72	0.5
		CALINE	0.67	0.47
		SIRANE	0.27	0.6
	<1 m/s	OSPM	0.48	0.42
		CALINE	0.19	0.375
		SIRANE	0.46	0.33

Also in former studies, when wind blew perpendicular to the road, both OSPM and CALINE models had better agreement with real world data (Kakosimos et al. 2010; Benson 1992; Levitin et al. 2005). To define perpendicularity, we conceived any angle bigger than 45 degrees between wind direction and road axis as perpendicular. In Table 7.5, obviously OSPM had better performance when wind blows perpendicularly to the road, comparing to both fixed-station and roadside measurement data. In contrast, SIRANE had similar performance in all wind direction conditions.

Table 7.5: Comparison between Wind Directions

Wind direction			FB	FAC2
Fixed-station	Perpendicular	OSPM	-0.15	0.8
		CALINE	-0.2	0.67
		SIRANE	-0.51	0.61
	Unperpendicular	OSPM	-0.34	0.75
		CALINE	-0.64	0.5
		SIRANE	-0.53	0.5
Roadside measurements	Perpendicular	OSPM	0.56	0.49
		CALINE	0.51	0.41
		SIRANE	0.2	0.43
	Unperpendicular	OSPM	0.58	0.46
		CALINE	0.27	0.5
		SIRANE	0.39	0.54

7.6 Conclusion

This chapter summarizes the results of the dispersion modeling chain and the model validation and inter-comparison. Traffic simulation reproduced the real-world traffic volume and composition well and provided solid foundation for emission calculation and dispersion modeling. Emission computation results cannot be validated against measured data and they were translated into emission factors to serve the models. Dispersion modeling results from the three models were visualized and compared with each other descriptively first and then validated against measured data using our evaluation system. The SIRANE model showed best overall performance amongst the three. Furthermore, it overcame the shortcoming of poor performance under paralleled wind. However, the three models still shared the disadvantage of poor performance under low wind speeds.

CHAPTER 8 CONCLUSION

8.1 Summary

Overall, the study elaborated in this thesis has achieved the two main objectives presented in Chapter 1. A state-of-the-art integration of microscopic traffic simulation, emission modeling, and air pollution dispersion was developed and used to simulate near-road NO_2 concentrations. With *in-situ* roadside measured and fixed-station NO_2 concentrations, the feasibility and performance of this 'dispersion modeling chain' was evaluated and validated.

With regards to the descriptive analysis of dispersion modeling results, several findings of interest are noted. We observed that compared to roadside measured data, fixed-station and simulated NO_2 concentrations fluctuated less and appeared to be much more stable. The concentration difference and weak correlation between roadside and fixed-station NO_2 concentrations justified the necessity of conducting on-site instantaneous monitoring, which can be useful for personal exposure research. There was a discrepancy between modeled and roadside measurements, which indicated that our dispersion modeling chain was not appropriate to simulate extreme events. However, it is feasible to use this methodology to predict and estimate long-time average (1-2 hours) and well-mixed NO_2 concentrations, as simulated values showed similar mean values and patterns against fixed-station data.

In addition to descriptive analysis, a set of performance measures including FB, NMSE, FAC2, MG, VG and NAD was used to parametrically evaluate the models' performance. The simulated results were first evaluated and compared for each road segment separately and then aggregately. The overall performance of our multi-model system was satisfying. It is worth noting that SIRANE had the best global performance, especially on segments 1 and 4 with buildings on both sides. In addition, the CALINE4 model, though not performing well in street canyon situations, had notably better agreement than the other two with roadside measurements when the surrounding built environment was similar to open terrain. Finally, the OSPM model had a moderate performance both in street canyon and open terrain situations. While all three models were unsuitable for conditions with lower or even calm wind speeds (<1 m/s), SIRANE was the only model that had stable performance under all wind directions.

8.2 Implications

This study is significant along two different dimensions: the methodological innovation in the dispersion modeling chain that allows air pollution modeling and the consequential takeaways for both policy makers and air pollution researchers.

First, second-by-second traffic conditions on the road network were simulated and employed for emission calculation. Unlike other studies that utilized traffic distribution and average traffic speed on the road links, this improvement enabled us to obtain more precise total emission results and thus better prediction of NO_2 concentrations. Secondly, the traffic, emission, and dispersion modeling results were collapsed into 8 simulation cases so that we can eliminate day-to-day variations in traffic and emissions, thus allowing us to better observe the effects of meteorology and the built environment. Finally, three dispersion models that have vast differences in their modeling algorithms were examined under the same meteorological, built environment and traffic conditions, using the same performance evaluation criteria.

In terms of results, this thesis may be relevant in two different fields of application. On one side, policy makers can find the results useful in the design of complete streets that minimize individuals' exposure to air pollution and in the placement of active transportation facilities such as cycling and pedestrian facilities. These findings shed light on those road configurations and meteorological conditions that are most and least prone to the dispersion of traffic-related air pollutants. On the other hand, this study contributes to the literature on air pollution research in terms of the performance of dispersion models under various land-uses and road geometries.

8.3 Limitations and Future Work

First of all, our data were collected from several different sources, on-site data measurements, and fixed-station data from weather and air quality stations. For instance, on-site NO_2 concentrations were averaged into one-hour intervals to accommodate fixed-station NO_2 data. Therefore, inevitably some information in the data would be omitted, e.g. instant concentrations spikes might be averaged off.

Secondly, additional sampling sites with various built environment characteristics should be selected in further studies, as during this campaign no road link with a high aspect ratio (H/W larger than 1) was examined.

Thirdly, the accuracy of dispersion models significantly depended on the background concentrations. It can be crucial to have valid local background concentrations. Thus, the results of this thesis can be difficult to reproduce in areas with inadequate air quality monitoring facilities.

Finally, sensitivity tests should be run in future studies to determine the impact of factors, such as wind profile and road configuration, that highly influences the performance of dispersion models.

REFERENCES

Abou-Senna, H., and E., Radwan. 2013. “VISSIM/MOVES Integration to Investigate the Effect of Major Key Parameters on CO2 Emissions.” *Transportation Research Part D: Transport and Environment* 21. Elsevier Ltd: 39–46. doi:10.1016/j.trd.2013.02.003.

Abou-Senna, H., E. Radwan, K. Westerlund, and C. D. Cooper. 2013. “Using a Traffic Simulation Model (VISSIM) with an Emissions Model (MOVES) to Predict Emissions from Vehicles on a Limit.” *Journal of the Air & Waste Management Association* 63:7, 819–31. doi:10.1080/10962247.2013.795918.

Alam, A., and M., Hatzopoulou. 2014. “Reducing Transit Bus Emissions: Alternative Fuels or Traffic Operations?” *Atmospheric Environment* 89. Elsevier Ltd: 129–39. doi:10.1016/j.atmosenv.2014.02.043.

Amirjamshidi, G., T. S. Mostafa, A., Misra, and M. J. Roorda. 2013. “Integrated Model for Microsimulating Vehicle Emissions, Pollutant Dispersion and Population Exposure.” *Transportation Research Part D: Transport and Environment* 18 (1). Elsevier Ltd: 16–24. doi:10.1016/j.trd.2012.08.003.

Aquilina, N., and A. Micallef. 2004. “Evaluation of the Operational Street Pollution Model Using Data from European Cities.” *Environmental Monitoring and Assessment* 95: 75–96. doi:10.1023/B:EMAS.0000029894.37253.dd.

Baldwin, N., O. Gilani, S. Raja, S. Batterman, R. Ganguly, P. Hopke, V. Berrocal, T. Robins, and S. Hoogterp. 2015. “Factors Affecting Pollutant Concentrations in the near-Road Environment.” *Atmospheric Environment* 115. Elsevier Ltd: 223–35. doi:10.1016/j.atmosenv.2015.05.024.

Beelen, R., G. Hoek, P. A. van den Brandt, R. A. Goldbohm, P. Fischer, L. J. Schouten, M. Jerrett, E. Hughes, B. Armstrong, and B. Brunekreef. 2007. “Long-Term Effects of Traffic-Related Air Pollution on Mortality in a Dutch Cohort (NLCS-AIR Study).” *Environmental Health Perspectives* 116 (2): 196–202. doi:10.1289/ehp.10767.

Beelen, R., M. Voogt, J. Duyzer, P. Zandveld, and G. Hoek. 2010. “Comparison of the Performances of Land Use Regression Modelling and Dispersion Modelling in Estimating Small-Scale Variations in Long-Term Air Pollution Concentrations in a Dutch

Urban Area.” *Atmospheric Environment* 44 (36). Elsevier Ltd: 4614–21. doi:10.1016/j.atmosenv.2010.08.005.

Benson, P. E. 1992. “A Review of the Development and Application of the CALINE3 and 4 Models.” *Atmospheric Environment Part B: Urban Atmosphere* 26 (3): 379–90. doi:10.1016/0957-1272(92)90013-i.

Berrone, S., F. De Santi, S. Pieraccini, and M. Marro. 2012. “Coupling Traffic Models on Networks and Urban Dispersion Models for Simulating Sustainable Mobility Strategies.” *Computers & Mathematics With Applications* 64 (6). Elsevier Ltd: 1975–91. doi:10.1016/j.camwa.2012.03.054.

Brauer, M., G. Hoek, H. A. Smit, J. C. de Jongste, J. Gerritsen, D. S. Postma, M. Kerkhof, and B. Brunekreef. 2007. “Air Pollution and Development of Asthma, Allergy and Infections in a Birth Cohort.” *European Respiratory Journal* 29 (5): 879–88. doi:10.1183/09031936.00083406.

Carpentieri, M., P. Salizzoni, A. Robins, and L. Soulhac. 2012. “Environmental Modelling & Software Evaluation of a Neighbourhood Scale , Street Network Dispersion Model through Comparison with Wind Tunnel Data.” *Environmental Modelling and Software* 37. Elsevier Ltd: 110–24. doi:10.1016/j.envsoft.2012.03.009.

Chang, J. C., and S. R. Hanna. 2004. “Air Quality Model Performance Evaluation.” *Meteorology and Atmospheric Physics* 87 (1-3): 167–96. doi:10.1007/s00703-003-0070-7.

Crouse, D. L., M. S. Goldberg, N. A. Ross, H. Chen, and F. Labrèche. 2010. “Postmenopausal Breast Cancer Is Associated with Exposure to Traffic-Related Air Pollution in Montreal, Canada: A Case-Control Study.” *Environmental Health Perspectives* 118 (11): 1578–83. doi:10.1289/ehp.1002221.

Environment Canada. 2013. *10 Years of Data from the National Air Pollution Surveillance (NAPS) Network, Data Summary from 1999 to 2008*. doi:Cat. No.: 978-1-100-54251-5. https://www.ec.gc.ca/rnspa-naps/77FECF05-E241-4BED-8375-5A2A1DF3688C/NAPS_Annual_Report_August2013_E

Felix, J. D., and E. M. Elliott. 2014. “Isotopic Composition of Passively Collected Nitrogen Dioxide Emissions: Vehicle, Soil and Livestock Source Signatures.” *Atmospheric Environment* 92 (x). Elsevier Ltd: 359–66. doi:10.1016/j.atmosenv.2014.04.005.

Gauderman, W. J., E. Avol, F. Lurmann, N. Kuenzli, F. Gilliland, J. Peters, and R. McConnell. 2005. “Childhood Asthma and Exposure to Traffic and Nitrogen Dioxide.” *Epidemiology* 16 (6): 737–43. doi:10.1097/01.ede.0000181308.51440.75.

Ghafghazi, G. 2014. “Simulating the Air Quality Impacts of Traffic Calming Schemes in a Dense Urban Neighbourhood.” *Transportation Research Part D: Transport and Environment* 7634. Elsevier Ltd: 11–22. doi:10.1016/j.trd.2014.11.014.

Hanna, S., and J. Chang. 2012. “Acceptance Criteria for Urban Dispersion Model Evaluation.” *Meteorology and Atmospheric Physics* 116 (3-4): 133–46. doi:10.1007/s00703-011-0177-1.

Hatzopoulou, M., and E.J. Miller. 2010. “Linking an Activity-Based Travel Demand Model with Traffic Emission and Dispersion Models: Transport’s Contribution to Air Pollution in Toronto.” *Transportation Research Part D: Transport and Environment* 15 (6). Elsevier Ltd: 315–25. doi:10.1016/j.trd.2010.03.007.

Holmes, N.S., and L. Morawska. 2006. “A Review of Dispersion Modelling and Its Application to the Dispersion of Particles: An Overview of Different Dispersion Models Available.” *Atmospheric Environment* 40 (30): 5902–28. doi:10.1016/j.atmosenv.2006.06.003.

Hülsmann, F., R. Gerike, and M. Ketzel. 2014. “Modelling Traffic and Air Pollution in an Integrated Approach – the Case of Munich” *Urban Climate* 10: 732–44. doi:10.1016/j.uclim.2014.01.001.

Jensen, S. S., T. Larson, K. C. Deepti, J. D. Kaufman, D. Heist, V. Isakov, S. Perry, et al. 2013. “Modeling Traffic Air Pollution in Street Canyons in New York City for Intra-Urban Exposure Assessment in the US Multi-Ethnic Study of Atherosclerosis and Air Pollution.” *Atmospheric Environment* 25 (30). Elsevier Ltd: 93–105. doi:10.1016/j.atmosenv.2009.06.042.

Kakosimos, K. E., O. Hertel, M. Ketzel, and R. Berkowicz. 2010. "Operational Street Pollution Model (OSPM) - A Review of Performed Application and Validation Studies, and Future Prospects." *Environmental Chemistry* 7: 485–503. doi:10.1071/EN10070.

Karim, A. A., and P. F. Nolan. 2011. "Modelling Reacting Localized Air Pollution Using Computational Fluid Dynamics (CFD)." *Atmospheric Environment* 45 (4). Elsevier Ltd: 889–95. doi:10.1016/j.atmosenv.2010.11.018.

Kenty, K. L., N. D. Poor, K. G. Kronmiller, W. McClenny, C. King, T. Atkeson, and S. W. Campbell. 2007. "Application of CALINE4 to Roadside NO/NO2 Transformations." *Atmospheric Environment* 41 (20). Elsevier Ltd: 4270–80. doi:10.1016/j.atmosenv.2006.06.066.

Kerckhoffs, J., M. Wang, K. Meliefste, E. Malmqvist, P. Fischer, N. a.H. Janssen, R. Beelen, and G. Hoek. 2015. "A National Fine Spatial Scale Land-Use Regression Model for Ozone." *Environmental Research* 140. Elsevier Ltd: 440–48. doi:10.1016/j.envres.2015.04.014.

Kim, Y., and J. Guldmann. 2015. "Land-Use Regression Panel Models of NO2 Concentrations in Seoul, Korea." *Atmospheric Environment* 107 (2). Elsevier Ltd: 364–73. doi:10.1016/j.atmosenv.2015.02.053.

Knibbs, L. D., M. G. Hewson, M. J. Bechle, J. D. Marshall, and A. G. Barnett. 2014. "A National Satellite-Based Land-Use Regression Model for Air Pollution Exposure Assessment in Australia." *Environmental Research* 135. Elsevier Ltd: 204–11. doi:10.1016/j.envres.2014.09.011.

Kukkonen, J., E. Valkonen, J. Walden, T. Koskentalo, P. Aarnio, A. Karppinen, R. Berkowicz, and R. Kartastenpää. 2001. "A Measurement Campaign in a Street Canyon in Helsinki and Comparison of Results with Predictions of the OSPM Model." *Atmospheric Environment* 35 (2). Elsevier Ltd: 231–43. doi:10.1016/S1352-2310(00)00200-4.

Levitin, J., J. Härkönen, J. Kukkonen, and J. Nikmo. 2005. "Evaluation of the CALINE4 and CAR-FMI Models against Measurements near a Major Road." *Atmospheric Environment* 39 (25). Elsevier Ltd: 4439–52. doi:10.1016/j.atmosenv.2005.03.046.

Lin, C., J. Gillespie, M.D. Schuder, W. Duberstein, I.J. Beverland, and M.R. Heal. 2015. "Evaluation and Calibration of Aeroqual Series 500 Portable Gas Sensors for Accurate

Measurement of Ambient Ozone and Nitrogen Dioxide.” *Atmospheric Environment* 100 (2). Elsevier Ltd: 111–16. doi:10.1016/j.atmosenv.2014.11.002.

Lin, D., X. Yang, and C. Gao. 2013. “VISSIM-Based Simulation Analysis on Road Network of CBD in Beijing, China.” *Procedia - Social and Behavioral Sciences* 96 (Cictp). Elsevier B.V.: 461–72. doi:10.1016/j.sbspro.2013.08.054.

Liu, W., X. Li, Z. Chen, G. Zeng, T. León, J. Liang, G. Huang, et al. 2015. “Land Use Regression Models Coupled with Meteorology to Model Spatial and Temporal Variability of NO2 and PM10 in Changsha, China.” *Atmospheric Environment*. Elsevier Ltd. doi:10.1016/j.atmosenv.2015.06.056.

Mead, M. I., O. M. Popoola, G. B. Stewart, P. Landshoff, M. Calleja, M. Hayes, J. J. Baldovi, et al. 2013. “The Use of Electrochemical Sensors for Monitoring Urban Air Quality in Low-Cost, High-Density Networks.” *Atmospheric Environment* 70. Elsevier Ltd: 186–203. doi:10.1016/j.atmosenv.2012.11.060.

Mensink, C., F. Lefebre, L. Janssen, and J. Cornelis. 2006. “A Comparison of Three Street Canyon Models with Measurements at an Urban Station in Antwerp, Belgium.” *Environmental Modelling & Software* 21 (4). Elsevier Ltd: 514–19. doi:10.1016/j.envsoft.2004.07.013.

Mensink, C., and Guido C. 2008. “From Traffic Flow Simulations to Pollutant Concentrations in Street Canyons and Backyards” *Environmental Modelling & Software* 23. Elsevier Ltd: 288–95. doi:10.1016/j.envsoft.2007.06.005.

Murena, F., G. Favale, S. Vardoulakis, and E. Solazzo. 2009. “Modelling Dispersion of Traffic Pollution in a Deep Street Canyon: Application of CFD and Operational Models.” *Atmospheric Environment* 43 (14). Elsevier Ltd: 2303–11. doi:10.1016/j.atmosenv.2009.01.038.

Parent, M. E., M. S. Goldberg, D. L. Crouse, N. A. Ross, H. Chen, M. F. Valois, and A. Liautaud. 2013. “Traffic-Related Air Pollution and Prostate Cancer Risk: A Case-Control Study in Montreal, Canada.” *Occupational and Environmental Medicine* 70 (7): 511–18. doi:10.1136/oemed-2012-101211.

Raducan, G. M. 2008. “Pollutant Dispersion Modelling with OSPM in a Street Canyon from Bucharest.” *Romanian Reports in Physics* 60 (4): 1099–1114.

Rood, A. S. 2014. “Performance Evaluation of AERMOD, CALPUFF, and Legacy Air Dispersion Models Using the Winter Validation Tracer Study Dataset.” *Atmospheric Environment* 89. Elsevier Ltd: 707–20. doi:10.1016/j.atmosenv.2014.02.054.

Shekarrizfard, M., M. Valois, M. S. Goldberg, D. Crouse, N. Ross, M. Parent, S. Yasmin, and M. Hatzopoulou. 2015. “Investigating the Role of Transportation Models in Epidemiologic Studies of Traffic Related Air Pollution and Health Effects.” *Environmental Research* 140. Elsevier Ltd: 282–91. doi:10.1016/j.envres.2015.04.002.

Sørensen, M., D. Hjortebjerg, K. T. Eriksen, M. Ketzel, A. Tjønneland, K. Overvad, and O. Raaschou-Nielsen. 2015. “Exposure to Long-Term Air Pollution and Road Traffic Noise in Relation to Cholesterol: A Cross-Sectional Study.” *Environment International* 85. Elsevier Ltd: 238–43. doi:10.1016/j.envint.2015.09.021.

Soulhac, L., P. Salizzoni, P. Mejean, D. Didier, and I. Rios. 2012a. “The Model SIRANE for Atmospheric Urban Pollutant Dispersion; PART II, Validation of the Model on a Real Case Study.” *Atmospheric Environment* 49 (39). Elsevier Ltd: 320–37. doi:10.1016/j.atmosenv.2011.11.031.

———. 2012b. “The Model SIRANE for Atmospheric Urban Pollutant Dispersion; PART II, Validation of the Model on a Real Case Study.” *Atmospheric Environment* 49. Elsevier Ltd: 320–37. doi:10.1016/j.atmosenv.2011.11.031.

Stevanovic, J., A. Stevanovic, P. T. Martin, and T. Bauer. 2008. “Stochastic Optimization of Traffic Control and Transit Priority Settings in VISSIM.” *Transportation Research Part C: Emerging Technologies* 16 (3). Elsevier Ltd: 332–49. doi:10.1016/j.trc.2008.01.002.

United States Environmental Protection Agency. 2012. “Motor Vehicle Emission Simulator (MOVES) User Guide for MOVES2010b.” http://www3.epa.gov/otaq/models/moves/documents/

United States Environmental Protection Agency. 2008. “Risk and Exposure Assessment to Support the Review of the NO 2 Primary National Ambient Air Quality Standard,” no. EPA-452/R-08-008a. http://www3.epa.gov/ttn/naaqs/standards/so2/data/200908SO2REAFinalReport

Vardoulakis, S., B. E. Fisher, K. Pericleous, and N. Gonzalez-Flesca. 2003. "Modelling Air Quality in Street Canyons: A Review." *Atmospheric Environment* 37 (2). Elsevier Ltd: 155–82. doi:10.1016/S1352-2310(02)00857-9.

Wallace, J., and P. Kanaroglou. 2008. "Modeling NOx and NO2 Emissions from Mobile Sources: A Case Study for Hamilton, Ontario, Canada." *Transportation Research Part D: Transport and Environment* 13 (5). Elsevier Ltd: 323–33. doi:10.1016/j.trd.2008.04.001.

Weichenthal, S., W. Farrell, M. Goldberg, L. Joseph, and M. Hatzopoulou. 2014. "Characterizing the Impact of Traffic and the Built Environment on near-Road Ultrafine Particle and Black Carbon Concentrations." *Environmental Research* 132. Elsevier Ltd: 305–10. doi:10.1016/j.envres.2014.04.007.

World Health Organization. 2013. "Review of Evidence on Health Aspects of Air Pollution – REVIHAAP Project," 309. http://www.euro.who.int/en/health-topics/environment-and-health/air-quality/publications/2013/review-of-evidence-on-health-aspects-of-air-pollution-revihaap-project-final-technical-report.

Wu, J., M. Wilhelm, J. Chung, and B. Ritz. 2011. "Comparing Exposure Assessment Methods for Traffic-Related Air Pollution in an Adverse Pregnancy Outcome Study." *Environmental Research* 111 (5). Elsevier Ltd: 685–92. doi:10.1016/j.envres.2011.03.008.

Xie, Y., M. Chowdhury, P. Bhavsar, and Y. Zhou. 2012. "An Integrated Modeling Approach for Facilitating Emission Estimations of Alternative Fueled Vehicles." *Transportation Research Part D: Transport and Environment* 17 (1). Elsevier Ltd: 15–20. doi:10.1016/j.trd.2011.08.009.

Zhang, K., and S. Batterman. 2013. "Air Pollution and Health Risks due to Vehicle Traffic." *Science of the Total Environment* 450-451: 307–16. doi:10.1016/j.scitotenv.2013.01.074.

Zhao, Y., and A. W. Sadeka. 2013. "Computationally-Efficient Approaches to Integrating the MOVES Emissions Model with Traffic Simulators." *Procedia Computer Science* 19. Elsevier B.V.: 882–87. doi:10.1016/j.procs.2013.06.118.